AN IVESTIGATION OF SOME AQUEOUS SOLUTION PROPERTIES OF DODECULAMMONIUM, N, N-DIMETHYLDODECYLAMMONIUM AND N, N, N-TRIMETHYLDODECYLAMMONIUM CHLORIDES

JOSEPH MARK MacNEIL

CANADIAN THESES ON MICROFICHE

I.S.B.N.

THESES CANADIENNES SUR MICROFICHE

National Library of Canada
Collections Development Branch

Canadian Theses on
Microfiche Service

Ottawa, Canada
K1A 0N4

Bibliothèque nationale du Canada
Direction du développement des collections

Service des thèses canadiennes
sur microfiche

NOTICE

The quality of this microfiche is heavily dependent upon the quality of the original thesis submitted for microfilming. Every effort has been made to ensure the highest quality of reproduction possible.

If pages are missing, contact the university which granted the degree.

Some pages may have indistinct print especially if the original pages were typed with a poor typewriter ribbon or if the university sent us a poor photocopy.

Previously copyrighted materials (journal articles, published tests, etc.) are not filmed.

Reproduction in full or in part of this film is governed by the Canadian Copyright Act, R.S.C. 1970, c. C-30. Please read the authorization forms which accompany this thesis.

AVIS

La qualité de cette microfiche dépend grandement de la qualité de la thèse soumise au microfilmage. Nous avons tout fait pour assurer une qualité supérieure de reproduction.

S'il manque des pages, veuillez communiquer avec l'université qui a conféré le grade.

La qualité d'impression de certaines pages peut laisser à désirer, surtout si les pages originales ont été dactylographiées à l'aide d'un ruban usé ou si l'université nous a fait parvenir une photocopie de mauvaise qualité.

Les documents qui font déjà l'objet d'un droit d'auteur (articles de revue, examens publiés, etc.) ne sont pas microfilmés.

La reproduction, même partielle, de ce microfilm est soumise à la Loi canadienne sur le droit d'auteur, SRC 1970, c. C-30. Veuillez prendre connaissance des formules d'autorisation qui accompagnent cette thèse.

THIS DISSERTATION
HAS BEEN MICROFILMED
EXACTLY AS RECEIVED

LA THÈSE A ÉTÉ
MICROFILMÉE TELLE QUE
NOUS L'AVONS REÇUE

NL-339 (r. 82/08)

Canada

AN INVESTIGATION OF SOME AQUEOUS SOLUTION PROPERTIES OF DODECYLAMMONIUM, N,N-DIMETHYLDODECYLAMMONIUM, AND N,N,N-TRIMETHYLDODECYLAMMONIUM CHLORIDES

by

© Joseph Mark MacNeil, B.Sc.

A Thesis submitted in partial fulfillment
of the requirements for the degree of
Master of Science

Department of Chemistry
Memorial University of Newfoundland

August, 1982

St. John's Newfoundland

ABSTRACT

Some aqueous micellar solutions of dodecylammonium chloride (DAC), dimethyldodecylammonium chloride (DMDAC) and trimethyldodecylammonium chloride (TMDAC) have been characterized by the methods of analytic equilibrium ultracentrifugation and variable shear viscometry in the presence of simple salt. In solutions of DAC the micelles become large and anisotropic with increasing concentration and ionic strength. Equilibrium centrifugation in 0.1 M NaCl shows that the micelles formed at the CMC are aggregates of only about 100 monomers but grow rapidly with increasing surfactant concentration until a larger micelle of about 350 monomers is formed. The size of the large micelles is extreamly sensitive to deprotonation and ionic strength but shows limited concentration dependence. The rheological characteristics of solutions of large micelles include a Newtonian region at low shear rates followed by an anomalous region in which the viscosity increases with increasing rate of shear. Shear thinning is observed at high shear rates. In contrast, a constant aggregation number of 100±10 has been obtained over a wide range of concentrations in solutions of DMDAC, TMDAC and some DAC-TMDAC mixtures at ionic strengths as high as 0.2 M. The same value is obtained in solutions of DAC at ionic strengths less than about 0.02 M. This remarkable result follows from an analysis

of the non-ideal behavior of these solutions in the centrifuge. The theory is based on a detailed description of the charge and salt effects, pair interactions and the macroscopic electric field which developes in the cell. Theoretical fit of the data also provides an estimate of an effective charge parameter which varies with ionic strength and head group in the order TMDAC>DMDAC>DAC. Intermediate values are obtained in mixed DAC-TMDAC solutions. Comparision of an estimated fractional surface charge, obtained by making Henry's correction to the charge parameter, with the values obtained from electrochemical measurements on solutions of large DAC micelles indicates that a critical value, above which large micelles will not form, is 0.25.

ACKNOWLEDGEMENTS

I would like to acknowledge the supervision of Dr. E. K. Ralph throughout the course of this research. Also, many thanks to Dr. P. D. Golding and Dr. J. M. W. Scott for their support. A special thanks to Mr. D. Hall for his guidance in the operation of the centrifuge.

TABLE OF CONTENTS

LIST OF TABLES

LIST OF TABLES (cont'd.)

LIST OF FIGURES

INTRODUCTION

Amphiphilic solute molecules aggregate in aqueous solutions to form colloidal particles called micelles when the concentration exceeds a value known as the critical micelle concentration[1,2], or CMC. Generally, if the amphiphile is a long chain alkyl surfactant containing a terminal ionizing head group, then, depending on the length of the hydrophobic tail and the nature of the hydrophilic head group, the micelles will be either small, probably spherical aggregates of less than 100 monomers or large, anisotropic aggregates of 100 to 10,000 monomers. In the former case the micellar mass is relatively insensitive to changes in ionic strength and surfactant concentration, while in the latter case it is strikingly dependent on both these parameters. Increasing alkyl chain length and decreasing head group size and degree of ionization favours the formation of large micelles.

The micelles that form in aqueous solutions of alkyl ammonium salts provide a good example of this variety in micellar behaviour. Data compiled by Tanford[3] from several sources[4,5,6] shows that the micellar mass for a series of these surfactants begins to increase as the length of the alkyl tail exceeds about 10 methylene units. This growth is dramatically affected by methylation of the ammonium head group, substitution of bromide for chloride counterion and the addition of simple electrolyte. For example, Kushner[5]

et, al. reported that the weight average aggregation number of dodecyl ammonium chloride in aqueous sodium chloride solutions at 30°C, increases from approximately 100 to 10,000 as the salt concentration is increased to 0.3 molar, while that of dodecyl trimethyl ammonium chloride increases from approximately 40 to 60 over the same range of salt concentration[6]. In the presence of 0.1 m NaCl at 30°C, decyl ammonium chloride has an aggregation number of 78; while in 0.5 m NaBr at 25°C, those of decyl ammonium bromide and decyl trimethyl ammonium bromide are 1100 and 48 respectively[4]. Such large changes in micellar size, due to what might appear to be very small changes in surfactant structure, have attracted theoretical attention for obvious reasons.

It is unfortunate, then, that the micellar aggregation numbers as measured by the usual techniques are almost invariably subject to some fundamental assumptions regarding the nature of these solutions. These include the assumption that upon extrapolating experimental results to the CMC, one obtains the result corresponding to infinite dilution of the macromolecule. This is strictly valid only when pre-CMC aggregation is negligible, and the degree of aggregation above the CMC is a simple monotonic function of the concentration in excess of the CMC. Otherwise, one obtains the aggregation number of what might cautiously be termed the hypothetical equivalent

micelle, which would produce the experimental results in concentrated solution. Micelles are intrinsically different in this regard than say biochemical macromolecules, in that their very existence depends on processes which occur only at finite concentrations. Also, there is always some uncertainty as to what value of the CMC to employ in these extrapolations, since it often varies with the property exploited in its evaluation.

Furthermore, such extrapolations usually weight data obtained in moderately concentrated solutions because of the experimental uncertainty associated with work close to the CMC. There are indications, however, that micellar behaviour is unusual in a range of concentration from the CMC to about twice this value[7]. The light scattering plots obtained by Attwood[8] for the nonionic detergent heptaoxyethylene glycol monohexadecyl ether show a pronounced curvature which suggests a bimodal distribution of micelles wherein the larger variety dominates at high concentration. Similarly, curved plots for decyl methyl ammonium bromide result in aggregation numbers of 270 to 670, depending on which concentrations the extrapolation is based[4].

Finally, it is often necessary to make large corrections to the experimental micellar mass on the basis of crude assumptions concerning the effect of solvent atmosphere, polydispersity, shape and particle interactions. For example, it has been popular to regard reduced specific

viscosities which are as much as two to three times larger than the intrinsic value given by Einstein[9] for spheres as being due to spherical micelles which are encompassed by a hydration layer which will reconcile this difference. However, it is equally plausible that at least some of this difference is due to anisotropy of the particle.

In a sophisticated investigation, Mazer et.al.[10] have concluded that sodium dodecyl sulphate micelles are best represented by a prolate shape. Their analysis involved comparing the temperature dependence of the light scattering intensity with the diffusion coefficient obtained by the quasielastic light scattering technique. In order to proceed with the analysis, it was assumed that the solutions containing large micelles were monodisperse even though the variance of the diffusion coefficient suggested the distribution of aggregation numbers extends 70% above and below the mean value. Also, in calculating mean aggregation numbers, it was implicitly assumed that the proportion of solvent atmosphere to micelle core remained constant independent of micelle size and shape. Preferential solvent interactions were ignored as was the effect of particle interactions. It was estimated that the latter effect would cause an error of about 12% in the mean particle radius. This corresponds to 40% of the volume and hence aggregation numbers of the limiting small micelle on which

all subsequent calculations were based. Still, this work represents one of the most thorough investigations of the effects of concentration, temperature and ionic strength on micellar mass and serves here as an example of how the determination of micellar mass is inextricably connected with an understanding of particle dynamics in solutions of polyelectrolytes.

In the present study, solutions of dodecyl ammonium chloride (DAC), dodecyl dimethyl ammonium chloride (DMDAC), dodecyl trimethyl ammonium chloride (TMDAC) and some mixtures of these surfactants were investigated using analytic ultracentrifugation and variable shear viscometry. Since its development by Svedberg[11], ultracentrifugation has become a widely used method for the identification and characterization of many macromolecular solutes[12,13]. Kratohvil[14], in his critical analysis of some techniques presently being used to determine micellar aggregation numbers, has endorsed the work of Doughty[15] who used equilibrium ultracentrifugation combined with isopiestic distillation to determine limiting aggregation numbers for sodium dodecyl sulfate micelles which are corrected for the effects of preferential solvent interactions. Interpretation of the effect in terms of a constant micellar charge resulted in values which are in agreement with those obtained from the electrophoretic mobility[16]. Unfortunately, Doughty did not

address the concentration dependence of the micellar mass, but did indicate that some extrapolated plots were curved. It will be shown, however, that an analysis of the concentration dependence of equilibrium centrifugation data can be used to obtain micellar parameters even when the solution is extremely non-ideal. The applicability of variable shear viscometry in assessing the rotational diffusion coefficient and hence shape of some large anisotropic micelles formed by DAC was also investigated.

When subjected to large centrifugal fields, buoyant micellar particles migrate toward the top of the centrifuge cell at a speed given by:

$$v = s\omega^2 r \qquad (1)$$

where s is the sedimentation coefficient, ω is the angular speed of the rotor and r is the distance from the center of rotation. When measured in ideal, dilute, incompressible solutions, s can be related to the buoyant mass of the particle, $\bar{M}$ and its friction coefficient, f, via[17]

$$s = \frac{\bar{M}}{f} \qquad (2)$$

Substitution of the Einstein[18] relation for the diffusion coefficient under these conditions,

$$D = \frac{RT}{f} \qquad (3)$$

where R is the gas constant and T is the temperature, results in the well known form of Svedberg's equation

for the molecular mass of the particle,

$$M = \frac{\bar{M}}{(1-\rho\bar{v})} = \frac{RT}{(1-\rho\bar{v})}\,\frac{s}{D} \qquad (4)$$

where ρ is the density of the solution and $\bar{v}$ is the partial specific volume of the micelle.

Independent determination of s and D by the common non-equilibrium methods[19] using a Schlieren optical system was found to be impractical in the alkyl ammonium chloride solution for a variety of reasons. The buoyancy factor for these surfactants is small so that, for the smaller micelles, the optimum field required for a sedimentation run was outside the range of the instrument. The larger micelles, on the other hand, exhibited self-sharpening Schlieren peaks characteristic of large anisotropic particles. This latter feature is primarily due to a markedly concentration dependent solution viscosity and has been successfully analyzed in the case of other anisotropic particles such as deoxyribonucleic acids and tobacco mosaic virus[20,21]. The concentration dependence of the micellar mass, however, complicates the interpretation of this phenomena in micellar solutions.

Evaluation of D by the synthetic boundary technique involves the centrifugal stabilization of a liquid-liquid interface between solutions of unequal density to obtain an initial step function concentration profile which is inevitably made uniform by diffusional flux. If these are two micellar solutions of slightly different

concentration then the temporal behaviour of the Schlieren pattern will be the simple error functions expected for a solute whose diffusion coefficient is intermidiate between those of the two solutions. Otherwise, the Boltzman-Matano procedure can be used to obtain the concentration dependence of D when two solutions of widely differing concentrations are used[22]. Attempts to obtain data by the former procedure were plagued by wave-like interfacial instabilities which were probably a consequence of the small density difference and hence slight centrifugal stabilization in these runs. Results obtained by the latter procedure were unreliable due to the compounded numerical error incurred when evaluating the necessary integrals when D varies rapidly with concentration and hence radial distance. The analysis could not be improved by allowing the Schlieren patterns to spread because of the physical limitations imposed by the walls of the centrifuge cell.

The bulk of the data in the present study was obtained during equilibrium experiments using the Archibald[23] or meniscus depletion[24] techniques. In the former, the fact that there is no mass flux through the ends of the liquid column in the centrifuge cell is applied as a boundary condition at any time after the start of rotation. The speed of rotation is chosen so as to cause a small but measurable perturbation of the solute distribution near the boundaries. In the latter the run is allowed to

proceed until the inevitable equilibrium distribution of all components is established throughout the cell. The analysis is facilitated by choosing a high rotational speed so that the cell will become devoid of solute at one end. In this case, the concentration profile is obtained directly from the integration of the Schlieren pattern.

Theoretical relationships for the analysis of equilibrium data have been derived for ideal systems from both the microscopic and macroscopic points of view. If the net flux of a component in the centrifuge cell is considered to be the result of an average velocity obtained by the individual particles under the separate influence of sedimentation and diffusion then,

$$J(r) = c(r)\ \langle v(r)\rangle = c(r)\left(\frac{\bar{M}\omega^2 r}{Nf} - \frac{k_B T}{f}\ \frac{d \ln c(r)}{dr}\right) \qquad (5)$$

where $J(r)$, $c(r)$ and $\langle v(r)\rangle$ are the flux per unit area, concentration, and average velocity of the solute particle at the radial position r, k_B is Boltzman's constant and N is Avogadro's number. At either end of the liquid column or throughout the cell at equilibrium the flux is zero and equation 5 reduces to:

$$\bar{M} = \frac{RT}{\omega^2 r}\ \frac{d \ln c}{dr} \qquad (6)$$

From thermodynamics the total chemical potential per mole of a component of an ideal solution in the centrifuge cell is given by the well known expression:

$$\mu = \mu_0 + RT \ln c - \bar{M}\omega^2 r^2/2 \qquad (7)$$

Equation 6 is obtained by recognizing that at equilibrium the gradient of equation 7 must vanish.

Determination of refractive index increments allows the right hand side of equation 6 to be derived from the Schlieren output to a good degree of approximation even when the dissolved particle is a polyelectrolyte so long as the refractive index increment is due mostly to the macroion which should be the case for long chain alkyl ammonium salts[25]. In the case of non-ideal solutions, equation 6 is used to define the apparent bouyant mass, $\bar{M}a$.

The value of $\bar{M}a$ obtained from centrifugation of micellar solutions will depend on many factors including pausidispersity due to the presence of free monomers as well as the possibility that the aggregates are polydisperse. Simple subtraction of the CMC from the total surfactant concentration circumvents errors caused by pausidispersity since the effect of the centrifugal fields on the low molecular mass monomers is negligible. Polydispersity in a self associating system represents a more fundamental problem since the general solution of the continuity equation for this case has not yet been developed. For this reason, data obtained using the Archibald technique is usually extrapolated to the time at which rotation was started so as to obtain parameters corresponding to the original distribution. Fujita et. al.[26] have discussed this problem in relation to dilute

solutions of polystyrene in methylethylketone and have pointed out that this feature can be mistaken for true thermodynamic non-ideality arising from particle interactions. In the system studied herein micelle-monomer dynamics are fast[27] compared to the relatively long time required to perturb the concentration during an equilibrium experiment so that the measured values of $\bar{M}a$ were independent of the time at which they were obtained.

Of a more serious impediment are those effects which are the result of electric charge on the micelle. The equations describing the formation of ionic species in an aqueous solution of monodisperse micelles, PY_z, and supporting electrolyte, XY, can be written

$$XY \rightarrow X^+ + Y^- \qquad (8)$$

$$PY_z \rightarrow P{Y_{(1-i)z}^{iz+}} + izY^-$$

where X^+ and Y^- are the coion and counterion respectively, z is the number of aggregated cationic surfactant monomers per micelle, P represents z surfactant cations and i is the charge parameter. Charge effects arise because of differential rates of sedimentation and diffusion of the ionic species present. The effect on sedimentation is particularly important in the micellar solutions studied because the buoyant macroions rise in the centrifugal field while the counterions tend to sink. Thus, an electric field develops between the top and bottom of the cell. Both species must sediment at an intermediate rate under

the influence of this electric field if the solution is to remain electrically neutral. In the case of diffusion, on the other hand, the migration of the macroions is actually enhanced by the electric field created by the more mobile counterions.

It is well known that the addition of simple salt will reduce the magnitude of this charge effect. Unfortunately, two new effects arise in such solutions. The primary salt effect is usually associated with conformational changes in protein systems. In micellar systems, the aggregation of monomers may also be dependent on ionic strength. A secondary salt effect caused by unequal mobilities of the simple ions is usually small[28].

There have been many theoretical efforts to describe the charge and salt effects since the development of centrifugal techniques. By considering the unequal electrophoretic mobilities of the ions present, Pedersen[29] was able to account for most of the charge effect in pure sedimentation. To do this, general equations for the velocity of each ion were solved simultaneously subject to the condition of electroneutrality. According to this analysis, an electric field develops in the cell as a result of a net displacement of the center of positive and negative charge associated with polarization between the sedimenting interface and the cell bottom. In essence, the electric field is assumed to vary inversely with

radial distance according to the application of Gauss's law to the case of two concentric infinite cylindrical tubes between which there is an electric potential difference[30].

Besides the condition of electroneutrality, all published analyses that explicitly recognize the presence of an electric field implicitly assume that edge effects in the finite centrifuge cell are negligible. In practice, this assumption might be expected to be valid so long as no convection is detected in the cell. Although there was no indication of convection in the experiments described here, it may be that the unusual patterns obtained by Anacker et.al.[31] for solutions containing DAC could be a result of convection due to this effect.

Alexandrowicz and Daniel[32,33] reanalysed the effect of charge on sedimentation and extended the analysis to include the case of pure diffusion by writing equations for the velocity of each ionic species in terms of the virtual velocities which would be obtained under the influence of just one of the forces acting on the kinetic particles. In the case of sedimentation these were the bouyant force due to the centrifugal field and an electrophoric force due to the electric field. The latter was expressed in terms of an effective charge on the ionic species rather than the electrophoretic mobility derived from other transport experiments used by Peterson. In

the case of pure diffusion the buoyant force was replaced by a chemical force due to the gradient of the chemical potential. By assuming a pseudo-ideal description of ionic activity they were able to derive rather complicated expressions for the apparent values of s and D of the macromolecule in terms of the bouyant mass, charge, concentration and frictional coefficients of the ionic species present.

The problem of simultaneous sedimentation and diffusion has been investigated using the methods of irreversible thermodynamics by Mijnlieff[34] and later by Varoqui and Schmitt[35]. More recently Eisenberg[28] has used irreversible thermodynamics to verify his reformulation of the Alexandrowicz-Daniel calculation wherein the buoyant forces on the ionic species were replaced by those acting on the electroneutral components only.

These theories adequately account for the charge and salt effect caused by the electric field which develops in the centrifugal cell during non-equilibrium experiments involving electrolytes. In most cases, their usefulness has been in choosing experimental conditions under which these effects would be negligible for the system in question. As a result, non-ideality due to particle interactions which would be expected when charge and salt effects are appreciable has been omitted. Also, as has been pointed out by Eisenberg[28], there has been confusion

concerning the identification of the apparent charge on the macromolecule derived from other transport experiments or the Donnan equilibrium experiment with the charge parameter required in these theories. More importantly, no attempt has been made to apply the results of these theories to the case of equilibrium centrifugation.

An analysis of equilibrium centrifugation in a system described by equation 8 which includes the effects of nonideality has been developed from a macroscopic thermodynamic approach by Lamm[36]. A simplified form of Lamm's equation is obtained by substituting the chemical activity of the electroneutral macromolecular component in equation 7 followed by the application of the equilibrium condition to give:

$$\bar{M}_{PY_z}\omega^2 r - RT\, d \ln a_{PY_z}/dr = 0$$

$$\bar{M}_{XY}\omega^2 r - RT\, d \ln c_{XY}/dr = 0 \qquad (9)$$

From electrochemistry,

$$a_{PY_z} = \gamma_{PY_z} c_P c_Y^{iz} \qquad (10)$$

where γ_{PY_z} is the c scale activity coefficient and the subscripts P and Y indicate the (1-i)z valent cation and the univalent anion respectively. Solving equations 9 subject to equation 10 and a statement of the electroneutrality condition,

$$c_Y = izc_P + c_X \qquad (11)$$

results in Lamm's equation,

$$\frac{RT}{\omega^2 r}\frac{d \ln c_p}{dr} = \bar{M}a = \frac{\bar{M}_{PY_z} - iz\bar{M}_{XY}c_X/(c_X + c_Y)}{1 + d \ln \gamma_{PY_z}/d \ln c_{PY_z} + (iz)^2 c_p/(c_X+c_Y)} \qquad (12)$$

This equation clearly illustrates the effect of non-ideality as well as charge on the measured molecular mass of a micellar particle obtained in an equilibrium centrifugation experiment. In dilute solutions, where $d \ln \gamma/d \ln c \to 0$, in the absence of simple electrolyte, $\bar{M}a$ will be only $1/(1 + iz)$ of $\bar{M}_{PY_z}$, while, even in the presence of simple electrolyte, extrapolation of $\bar{M}a$ values to infinite dilution will result in an underestimation of the true mass by $izM_{XY}/2$. It is convenient to identify the terms in the right hand side of equation 12 with the various effects. Hence, the second term in the numerator is the salt term, the second term in the denominator is the non-ideality term and the third is the charge term.

Several electrochemical techniques have developed since the original treatment by Maxwell[37] of the problems arising when the passage of an electric current is associated with the transfer of relatively massive particles of ions. These include those which measure the response of charged particles to an applied electric field as well as some which record the electric field spontaneously arising in a system throughout which the centrifugal potential varies. In his early work, Tolman[38] was able to calculate transference numbers

from the initial difference in electric potential measured across the ends of a rotating tube containing an aqueous electrolyte. In his experiments this difference was measured well before a significant concentration change occured in the rotating tube. Tolman suggested that this electric potential difference would eventually vanish as the inevitable equilibrium distribution of the charged species was established. The fact that a term due to the electric field is not explicitly included in Lamm's equation may have served to perpetuate this view. It will be shown in the theory section, however, that a microscopic analysis similar in some respects to that of Alexandrowicz and Daniel which both explicitly incorporates a virtual velocity due to the electric field and also includes the effects of non-ideality by recognizing the influence of particle interactions on the average velocity of the charged macromolecule results in an equation for centrifugal equilibrium analogous in form to Lamm's. The assumption embraced by adopting the electroneutrality condition is considered as is the relationship between the centrifugal and electric field strengths. The latter suggests that measurement of the electric field during centrifugation would provide useful information concerning the charged species. Furthermore, the charge parameter of the macroion will be given a precise kinetic definition which allows for comparison with that obtained from other techniques. The equation has the

added benefit of a sound theoretical basis on which to calculate the magnitude of the non-ideality term in centrifugation experiments.

In order to complete the centrifugal analysis, it was necessary to evaluate the partial specific volume, and hence buoyancy factor, of the surfactants used as well as the specific refractive index increment for use in the interpretation of Schlieren patterns. Also, the CMC of DMDAC at various ionic strengths was established using the surface tension method. This data supplements literature values available for DAC and TMDAC[39].

The large micelles that form in solution of DAC at relatively low ionic strength were investigated by measuring the shear dependence of the solution viscosity. The intrinsic viscosity, or shape factor, of a solute in solution is defined by,

$$\nu = \eta_{sp}/\phi \qquad (13)$$

where ϕ is the volume fraction of the hydrodynamic solute particles and η_{sp} is the specific viscosity given in terms of the solution viscosity, η, and the solvent viscosity, η°, by[40]

$$\eta_{sp} = \eta/\eta_{o} - 1 \qquad (14)$$

When measured in solutions of non-interacting, rigid particles, and at low rates of shear, ν is related to the shape of the solute particles[41], while its non-Newtonian dependence on the shear rate is related to both the size

and shape of the particle via the rotational diffusion coefficient.[42,43,44] Normally, ν cannot be calculated from experimental results without assuming a relationship between ϕ and the solute concentration, c, which corrects for the possibility that the shear surface surrounding the particle may encompass solvent molecules which are carried along with the particle. For this reason, it is usually the reduced specific viscosity, η_{sp}/c, which is reported.

The reduced specific viscosity measured at low rates of shear has often been used to characterize micellar solutions in which the electroviscous effect[45] has been reduced by the addition of simple salt. In particular, Kushner[5] has measured the low shear viscosity of DAC solutions containing various amounts of salt and has found that the reduced specific viscosity increases with increasing ionic strength. These results have been interpreted by Stigter[46] in terms of a theory[47] for flexible rod-like micelles while Tanford[3] has suggested that the same data concurs with the growth of rigid, oblate ellipsoidal micelles. Interestingly, Stigter begins his earlier argument by pointing out the lack of agreement between the experimental viscosity and the theoretically predicted values which are based on either prolate or oblate ellipsoidal shapes. When the present work was undertaken, it was hoped that the question of the shape of large DAC

micelles could be resolved by observing the shear dependence of the reduced specific viscosity since this should be quite different for the different model shapes proposed.

THEORY

If the average velocity of a micellar particle in the centrifuge is approximated by a linear combination of hypothetical velocities due to centrifugal, stochastic, and electrophoretic velocities written explicitly as forces divided by frictions where the electric force arises because of both particle interactions and also the presence of a macroscopic electric field, then the radial flux of these particles is given by,

$$J = c\langle v \rangle = c\left(\frac{\bar{M}\omega^2 r}{Nf} - \frac{k_B T}{f}\frac{d \ln c}{dr} + \frac{F}{f} + \frac{Q}{f}E\right) \qquad (15)$$

where N is Avogadro's constant, k_B is Boltzman's constant, F is the force due to particle interactions, E is the macroscopic electric field, Q is the effective ionic charge on the micelle, and the brackets indicate a configurational average of the quantities enclosed. In an important paper on the diffusive transport of charged macromolecules, Anderson and Reed[48] have clearly established that separate averaging of the interparticle force and the frictional coefficient constitutes a substantial theoretical error since these forces are usually appreciable at small interparticle distances for which the average bulk frictional coefficient is a poor approximatation to a more realistic analysis of the hydrodynamic interactions which would occur. Therefore, following their general approach, if the forces in equation 15 are assumed to be uncorrelated, extraction of a factor

representing a configurational average inverse frictional coefficient gives,

$$J = c\langle f^{-1}\rangle\left[\frac{\bar{M}\omega^2 r}{N} - k_B T \frac{d \ln c}{dr} + \left\langle\frac{1}{f}\right\rangle^{-1}\left\langle\frac{F}{f}\right\rangle + QE\right] \qquad (16)$$

By considering binary interactions of spherical particles, Anderson and Reed have derived a relationship between the third term in equation 16 and the macroscopic concentration gradient included in the second term which should be accurate in dilute solutions. Accordingly, equation 16 becomes,

$$J = c\langle f^{-1}\rangle\left[\frac{\bar{M}\omega^2 r}{N} - k_B T \frac{D}{D^*} \frac{d \ln c}{dr} + QE\right] \qquad (17)$$

where D/D^* is the ratio of mutual and tracer diffusion coefficients of the particle.

According to their theory this ratio is given by,

$$\frac{D}{D^*} = \frac{1 + 8(I - \Lambda)\phi}{1 - 8\Lambda\phi} \qquad (18)$$

where ϕ is the hydrodynamic volume fraction of the solute, and I and Λ can be calculated from the interaction energy, W, and hydrodynamic parameters, τ and K, via the following equations,

$$I = -(k_B T)^{-1} \int_0^\infty \frac{(1+\rho)}{\tau(\rho)} \frac{dW(\rho)}{d\rho} \exp-(W(\rho)/k_B T)\, d\rho \qquad (19)$$

$$\Lambda = \int_0^\infty (1+\rho)^2 \, k(\rho) \exp-(W(\rho)/k_B T)\, d\rho \qquad (20)$$

In these equations ρ is the reduced interparticle separation given in terms of the center to center distance, r, and the particle radius, a, by,

$$\rho = r/2a - 1 \qquad (21)$$

The function $\tau(\rho)$ arises from consideration of the problem of two equivalent spheres translating either toward or away from each other at equal speeds solved by Rushton and Davies[49]. For numerical purposes, it is approximated by,

$$\tau = 1 + b\rho^{-c} \tag{22}$$

where

$b = 0.2715$ $c = 0.989$ for $0.000001 < \rho < 0.013$

$b = 0.5510$ $c = 0.812$ for $0.013 < \rho < 2.3$

$b = 0.6933$ $c = 0.989$ for $2.3 < \rho < \infty$

The function $\kappa(\rho)$ is a more complicated result associated with the response of a Brownian particle to fluctuating solvent forces in the presence of neighboring particles. A formalism developed by Batchelor[50] allows $K(\rho)$ to be derived from hydrodynamic calculations in the literature. Figure 4 of reference 48 contains the necessary data for numerical work.

Using these results we can describe the flux in the system given by equation 8 by application of equation 16 to each of the charged species,

$$J_p = c_p \langle f_p^{-1} \rangle \left[\frac{\bar{M}_p \omega^2 r}{N} - k_B T \frac{D}{D^*} \frac{d \ln c_p}{dr} + izE \right] \tag{23a}$$

$$J_Y = c_Y \langle f_Y^{-1} \rangle \left[\frac{\bar{M}_Y \omega^2 r}{N} - k_B T \frac{d \ln c_Y}{dr} - E \right] \tag{23b}$$

$$J_X = c_X \langle f_X^{-1} \rangle \left[\frac{\bar{M}_X \omega^2 r}{N} - k_B T \frac{d \ln c_X}{dr} + E \right] \tag{23c}$$

where it has been assumed that D/D^* for the univalent species is unity. These equations simplify at centrifugal equilibrium, or at the ends of the liquid column, to

$$\frac{\bar{M}_P\omega^2 r}{N} - k_B T \frac{D}{D^*} \frac{d \ln c_P}{dr} + izE = 0 \qquad (24a)$$

$$\frac{\bar{M}_Y\omega^2 r}{N} - k_B T \frac{d \ln c_Y}{dr} - E = 0 \qquad (24b)$$

$$\frac{\bar{M}_Y\omega^2 r}{N} - k_B T \frac{d \ln c_X}{dr} + E = 0 \qquad (24c)$$

In general, this system of simultaneous differential equations must be solved subject to Gauss' law for the electric potential, ψ, in a cylindrical coordinate system given by[30],

$$\frac{d}{dr}\left(r \frac{d\psi}{dr}\right) = iz c_P + c_X - c_Y \qquad (25)$$

and would result in more or less independent radial distributions of $PY^{iz+}_{(1-i)_z}$, Y^- and X^+. Recognition of the fact that electric forces between ions are generally much stronger than the centrifugal force applied even in the ultracentrifuge leads to the adoption of the electroneutrality condition in the bulk of the solution,

$$izc_P + c_X - c_Y = 0 \qquad (26)$$

It follows from equation 25 that in this case the electric field, $E = d\psi/dr$, will vary with r^{-1} between the ends of the liquid column consistent with the presence of equal but opposite polarization charges at these surfaces.

Equations 24 can be solved by substituting equation 26 in 24a, followed by 24b and 24c, to obtain,

$$\frac{\omega^2 r\bar{M}_P}{N} + izE - \frac{D}{D^* izc_P}\left[c_Y\left(\frac{\omega^2 r\bar{M}_Y}{N} - E\right) - c_X\left(\frac{\omega^2 r\bar{M}_X}{N} + E\right)\right] = 0 \qquad (27)$$

This can be rearranged to obtain a relationship for the ratio of electric and centrifugal fields,

$$\frac{NE}{\omega^2 r} = \frac{(-izc_p\bar{M}_p D^*/D + c_Y \bar{M}_Y - c_X\bar{M}_X)/(c_X+c_Y)}{D/D^* + (iz)^2 c_p/(c_X+c_Y)} \qquad (28)$$

Substitution of equation 28 in 24a leads to an expression for the apparent buoyant molecular mass of the macromolecule,

$$\frac{RT}{\omega^2 r}\frac{d \ln c_p}{dr} = \bar{M}a = \frac{\bar{M}_p + iz(c_Y\bar{M}_Y - c_X\bar{M}_X)/(c_X+c_Y)}{D/D^* + (iz)^2 c_p/(c_X+c_Y)} \qquad (29)$$

which can be rewritten in terms of the buoyant molecular mass of the neutral species defined by,

$$\bar{M}_{PY_z} = \bar{M}_P + iz\bar{M}_Y \qquad (30)$$

and

$$\bar{M}_{XY} = \bar{M}_X + \bar{M}_Y \qquad (31)$$

to give the desired result,

$$\bar{M}a = \frac{\bar{M}_{PY_z} - iz\bar{M}_{XY}c_X/(c_X+c_Y)}{D/D^* + (iz)^2 c_p/(c_X+c_Y)} \qquad (32)$$

It should be noted that D/D^* obtained in this analysis is not given by the concentration dependence of the activity coefficient of the macromolecule as given by classical theory,[13]

$$D/D^* = 1 + d\ln\gamma/d\ln c \qquad (33)$$

If this expression is equated with the deviation from ideality of the concentration dependence of the osmotic pressure, then[51]

$$\frac{d \ln \gamma}{d \ln c} = \frac{-4\pi c}{3} \int_0^\infty g \frac{dW}{dr} r^3 dr \qquad (34)$$

where g is the radial distribution function. Integration of equation 34 will clearly give different results than those obtained via equation 18. Some of the limiting relationships concerning this matter are discussed in Anderson and Reed's paper.

Hence, Lamm's choice of electroneutral species as thermodynamic components and the subsequent adoption of the electroneutrality condition are, in the strictest sense, redundant and, in general, neither can be assumed rigorous in the analysis of the centrifugal equilibrium. The fact that the electric field strength is not explicitly included in Lamm's equation does not indicate that it vanishes at equilibrium but only that it varies as r^{-1} between the top and bottom of the liquid column. The suggestion by Cassassa and Eisenberg[52] that the electric field is "inconsequential" is fortuitously accurate in as much as the general form of Lamm's equation includes the major effects due to the existence of this field as can be seen from a comparison of equation 32 with equation 12, so long as the non-ideality term is calculated correctly. To complete this argument, consider the form of equation 24 if we were to insist that the electric field vanish. From equation 24a,

$$\frac{RT}{\bar{M}_a} \frac{d \ln c_p}{dr} = \bar{M}_a = \bar{M}_p \frac{D^*}{D} \qquad (35)$$

clearly in disagreement with equation 12.

Finally, evaluation of the magnitude of the electric field by introducing typical parameter values into equation 28 suggests the plausability of developing an analytical technique based on its measurement. Anticipating some results for the alkyl ammonium chloride micelles suggests introducing 0.5, 100 and 2000 g mol^{-1} for i, z, and $\bar{M}_P$ respectively while typical run conditions given zc_P=0.05 M; c_X=0.1 M; ω=2,000 s^{-1}; r=7.0 cm; and if we assume $c_X\bar{M}_X \cong c_Y\bar{M}_Y$ and D*/D=0.5 then E becomes 10^{-15} dynes esu^{-1} and the theoretically measurable electric potential difference across a 1 cm liquid column is approximately 0.5 mV.

EXPERIMENTAL

Materials: Dodecylammonium chloride, DAC, (Eastman Kodak) was recrystalized twice by addition of 500 ml diethyl ether to 100 ml of warm ethanol solution containing 30 g of the surfactant followed by cooling. Dimethyldodecylammonium chloride, DMDAC, prepared from a purified sample of the tertiary amine (Eastman Kodak) and subsequently recrystalized several times from dry ethyl acetate was kindly supplied by Dr. P. Golding. Trimethyldodecylammonium chloride, TMDAC, (Eastman Kodak) was recrystalized twice from warm, freshly azeotroped benzene by addition of small portions of petroleum ether followed by cooling. All surfactants were stored over anhydrous silica gel in a vacuum desiccator. Sodium chloride (Fisher, certified ACS), potassium chloride (BDH, certified ACS), sodium hydroxide (Fisher, certified ACS) and hydrochloric acid (Anachemia, Standard Volumetric Solution) were used without further purification. Dr. P. Golding also supplied a purified sample of sucrose. Solutions were made using doubly distilled water. The second distillation being from a Barnstead Water Still equipped with a borosilicate condenser.

Surface Tension Measurements and CMC's: The equilibrium surface tension of DMDAC solutions were determined by the bubble pressure method using a pyrex capillary tube (7mm) drawn down to about 2 mm and submerged about 1 cm below the flat surface of the solution. The temperature of the solution was maintained at 30.00 ±0.05°C by circulating water through the Dewar walled sample beaker and was monitored with a copper-constantan thermocouple placed in close proximity to the bubble. The solution was stirred between measurements.

The equilibrium pressure difference across the air-liquid interface was obtained in the following way. The system was pressurized by incrementally advancing the plunger of a 5 ml syringe containing air and connected to the capillary tubing until a continuous stream of bubbles was observed. Then, with the volume of the system fixed, the detachment of individual bubbles was monitored with a MKS Capacitance Pressure Manometer fitted with a 0-100 mmHg head. Since the volume of the system had been minimized the reduction in pressure due to each bubble was clearly observable until finally the critical value corresponding to the surface tension of the equilibrium interface was established after which bubbles no longer separated from the capillary tip.

In this way a pressure difference of 36,5 mmHg was recorded with pure water after corrections for the

hydrostatic head, yielding a calibration constant of 1.951 dynes $cm^{-1} mmHg^{-1}$.[53] The dependence of the surface tension on the concentration of surfactant was obtained by adding small amounts of a concentrated stock solution. Because of the small size of the bubbles formed and the lack of flow during the final measurement, the corrections for gravity effects and complications due to viscous drag common to this technique were avoided[54].

Surface tensions at various molar concentrations of DMDAC for the three KCl concentrations investigated are listed with the data in table 6. CMC's were obtained as the intercept of a line fitted to the constant, high concentration tensions and a non-linear fit[55] of the low concentration tensions based on equation 36 which is derived from standard considerations of the kinetics of surface coverage, and surface excess[54].

$$\gamma = \gamma_o - \frac{RT}{k_3} \ln (1 + \frac{k_1}{k_2} c) \qquad (36)$$

In this equation γ is surface tension, γ_o is the surface tension of pure water, k_1 and k_2 are rate constants for diffusion on and off the surface respectively and k_3 is the proportionality constant relating surface excess and fractional surface coverage. The fits resulted in values of 16.2 dynes cm^{-1}, 8.86 dynes cm^{-1} and 8.87 dynes cm^{-1} for RT/k_3, and 490 M^{-1}, 7230 M^{-1} and 17000 M^{-1} for k_1/k_2 for solution containing 0.00 M, 0.0393 M and

0.1429 M KCl respectively. A log-log plot of CMC vs total chloride concentration resulted in -0.618 ±0.007 and -2.993 ±0.011 for the parameters a and b in equation 37.

$$\log \text{CMC} = a \log [Cl^-] + b \qquad (37)$$

When required, CMC's of DAC and TMDAC were obtained from similar fits to published CMC's[56].

Density Measurements and Partial Specific Volumes:

Densities required to calculate the hydrostatic head for the viscosity experiments were determined using a 10 ml picnometer. More precise data was required to evaluate the buoyancy factor for the analysis of centrifuge data. Therefore, the densities of solutions of DAC, DMDAC, TMDAC and a mixture of DAC and TMDAC in 0.1M NaCl were determined using the apparatus depicted in figure 1. This consisted of a ballasted quartz bulb suspended from a quartz spring whose force constant was approximately 10 dynes cm^{-1}. Both the bulb and spring were completely submerged below the air-liquid interface so that the correction for the effect of surface tension typical of buoyant methods was avoided. The outside water jacket was thermostated at 30.00 ±0.01°C and ample time was allowed for thermal equilibration of each solution. The extension of the spring E was measured with a linear microscope capable of resolving 0.01 mm.

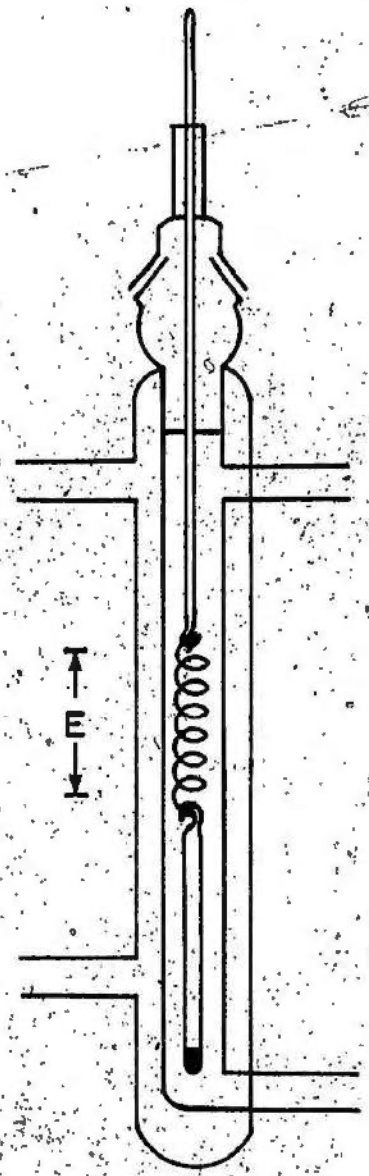

Figure 1 Density apparatus showing the measured extension (E) of the quartz spring.

Because of the fragile nature of the glass spring only liquids with low surface tensions were added directly to the dry apparatus. A series of measurements was initiated by filling the apparatus with a surfactant solution whose concentration was approximately equal to the CMC. The surfactant concentration was increased by adding solid to the stock solution and, in a cyclic fashion, displacing the former solution until further additions resulted in no change in E thereby obtaining data at constant moles of solvent. Similarly, the calibration runs with aqueous NaCl solutions were initiated by filling with acetone followed by displacement by large quantities of the calibrating solution. Finally, E was measured three times with the supporting hook in different locations along the vertical axis of the apparatus. The consistency of the results obtained indicate that the glass walls of the jacketed tube were free from distortion and the solution composition and temperature were uniform.

The density of the calibrating solutions were calculated by the well known equation for dilute electrolytic solutions[57].

$$\rho = \rho_o + (M - \rho_o \phi_V^o)\, c/1000 - S_V \rho_o c^{3/2}/1000 \qquad (38)$$

where M is the molecular mass of NaCl and ϕ_V^o and S_V are given by the concentration dependence of the apparent

molar volume,

$$\phi_V = \phi_V^0 + S_V c^{\frac{1}{2}} \qquad (39)$$

and c is the molar concentration of NaCl. The values of 0.995680, 16.91 and 2.024 for ρ_0, ϕ_V^0 and S_V respectively at 30.00°C were derived from parabolic interpolation of the data of Baxter and Wallace[58] at 0.00°C, 25.00°C and 50.04°C. The concentrations in units of c were derived from molal values, m, from equation 40 using a transcendental procedure.

$$c = m\rho_0(1 - c\phi_V/1000) \qquad (40)$$

Linear least square regression of the proposed calibration equation,

$$\rho = aE + b \qquad (41)$$

yielded -6.292×10^{-4} and 1.037744 for the parameters a and b respectively. From the residues of this fit listed in table 1 it is inferred that this equation adequately describes the data and that the standard error in experimental values of ρ are in the order of 10^{-5} grams cm^{-3}. The measured densities for various molal concentrations of surfactant are listed with the data in tables 7 through 10.

To obtain partial specific volumes a non-linear fit[55] of the data to the semi-empirical equation,

$$\rho = A + Bm_2 + Cm_2^{3/2} \qquad (42)$$

was used to evaluate the necessary terms in the defining

TABLE 1

CALIBRATION OF DENSITY APPARATUS WITH SOLUTIONS OF NaCl AT 30.00°C

m	ρ(g/ml)	Σ(mm)	$(\rho-\rho_{calc})^* \times 10^5$
0	.995676	66.850	- .7
.02494	.996705	65.213	- .8
.04941	.997703	63.643	.2
.09916	.999718	60.460	1.4
.1487	1.001710	57.280	.6
.1978	1.003671	54.137	-1.1

*Calculated using equation 41

equation,

$$\bar{v} = \frac{1}{\rho} - \frac{1000 + m_2M_2 + m_3M_3}{M_2\rho^2} \left(\frac{\partial \rho}{\partial m_2}\right)_{P,T,m_1,m_3} \qquad (43)$$

where the subscripts 1, 2 and 3 refer to H_2O, surfactant and NaCl respectively. As all the elements of the error co-variance matrix, σ_{ij}, are obtained from this fit it is possible to compute the concentration dependence of the partial specific volumes along with error curves which represent the total propagated error[55]. The fit parameters are found in table 2 while the partial specific volumes are shown in figure 2. From these plots it is apparent that the partial specific volumes of DAC, DMDAC and TMDAC have the constant values of 1.0955 ml g^{-1}, 1.1055 ml g^{-1} and 1.0975 ml g^{-1} respectively over the range of concentration investigated. Also, the mixture of DAC with TMDAC for which the partial specific volume is 1.0965 ml g^{-1} demonstrates that for mixtures it can be calculated as the mole fraction weighted sum of the above values.

It is noteworthy that less rigorous evaluations of partial specific volumes almost invariably result in systematic variation with concentration[59]. Also, in this work, the curves were not affected by a change in $\bar{v}$ at the CMC since in all solutions the surfactant concentration was greater than the respective CMC's. Because of this, the parameter A in table 2 is not expected to agree with the value of ρ_o used in equation 38.

TABLE 2

PARAMETERS AND ERRORS OF FIT OF DENSITY DATA TO EQUATION 42.

	DAC	DMDAC	TMDAC	$X_{DAC}/X_{TMDAC} = .924$
m of NaCl	.1010	.1002	.0996	.1003
A	.999819	.999777	.999737	.999747
$-B \times 10^{2}$	1.951	2.649	2.663	2.299
$C \times 10^{3}$	4.589	3.283	5.775	3.896
$\sigma_{AA} \times 10^{11}$	46.92	7.313	8.855	4.099
$\sigma_{BB} \times 10^{7}$	53.39	2.792	5.992	1.123
$\sigma_{CC} \times 10^{7}$	764.8	21.67	61.59	6.791
$-\sigma_{AB} \times 10^{9}$	48.56	4.000	6.473	1.846
$\sigma_{AC} \times 10^{9}$	179.6	10.42	19.45	4.212
$-\sigma_{BC} \times 10^{7}$	201.2	7.709	19.04	2.732

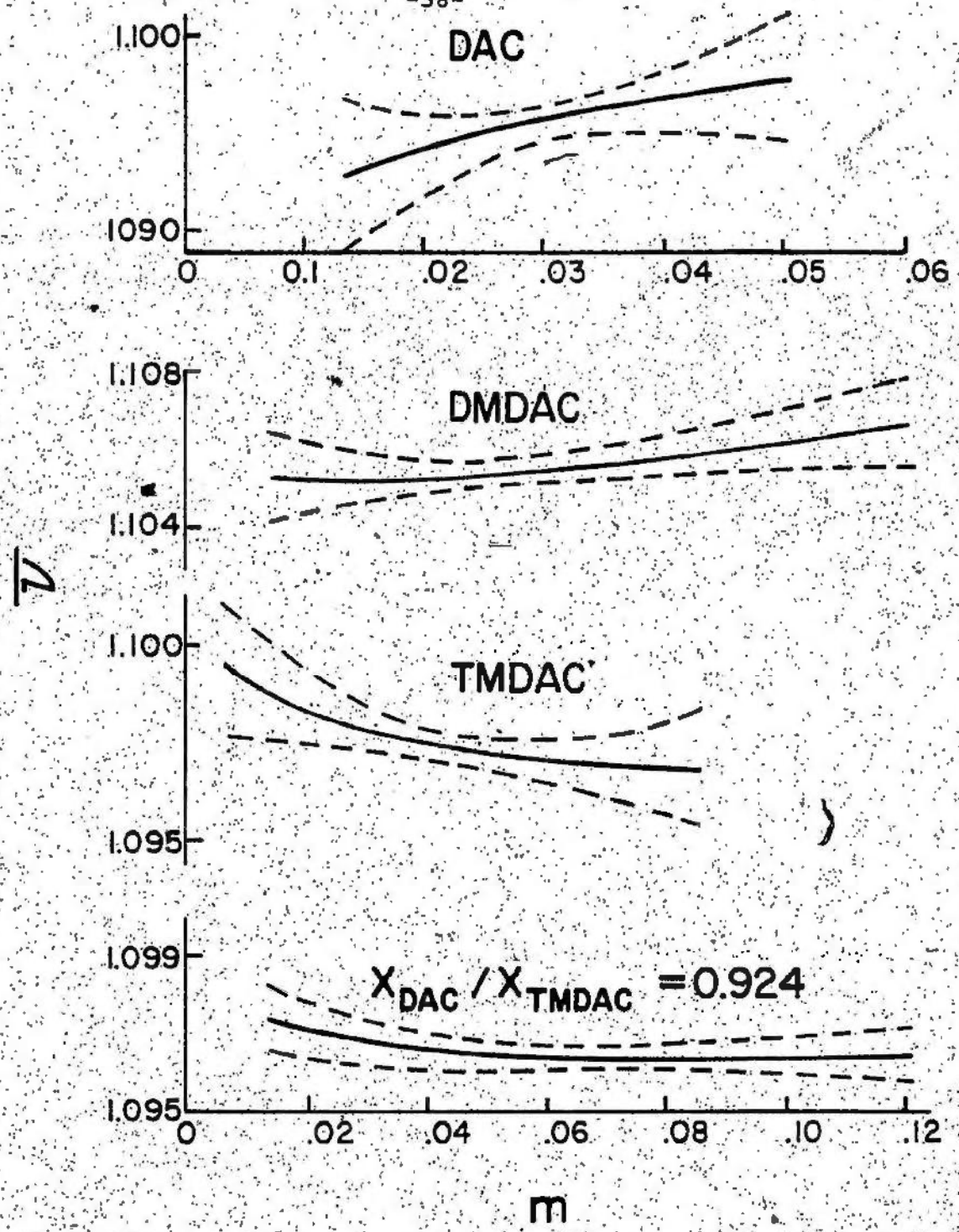

Figure 2 Partial specific volumns (cm^3/g) vs. molality of surfactant in 0.1 M NaCl. Error curves are dashed.

Refractive Index Measurements and Specific Refractive Index Increments: Refractive indices were determined with a Pulfrich refractometer # 602701 made by Bellingham and Stanley Limited. The special cell supplied by the manufacturer was modified by adding teflon gaskets to prevent syphoning of the solutions along the ground glass side walls and the prism. A cover fitted with a thermocouple minimized the risk of contamination. A circulating bath connected to the cell's integral water jacket maintained the sample temperature at 20.00 ±0.01°C in a room thermostated at 20.0 ±0.1°C. The sodium lamp used provided lines at 498.8 nm, 568.5 nm, and 615.8 nm which were intense enough to permit determination of the refracted angle to within 5" of arc.

Calibration involved determining the index of the prism, $N(\tau)$, at the four wavelengths used. The calibrating fluid was water for which dispersion data[60] yields a value of $8.10 \pm 0.05 \times 10^3 nm^2$ for the parameter B in equation 44,

$$n^2 - n_D^2 = B(1/\tau^2 - 1/\tau_D^2) \qquad (44)$$

which adequately represents the dispersion data in the visible region about the index found using the sodium D line, τ_D, at 589.2 nm. Hence $N(\tau)$ could be calculated via the equation of the instrument,

$$n^2 = N^2 - \sin\theta\,(N^2 - \sin^2\theta) \qquad (45)$$

Equation 45 was then used to calculate experimental indices from the refracted angle θ.

The refractive indices are included with the data in table 11. Linear least squares fit of the data result in specific refractive increments listed in table 3.

Centrifugation: A Beckman Model E Analytic Ultracentrifuge equipped with a phase plate was employed in these investigations. The light source was a mercury arc lamp fitted with a wratten 77A filter transmitting the line at 546.0 nm. Schlieren patterns were recorded on Kodak Melallographic plates and analysed with a Nicon Model 6C Profile Projector. The standard procedure of scaling by the ratio of the distance between radial reference marks in the cell to the measured distance between the respective marks on the photographic plates was used.

Calibration of the optical system was performed during a synthetic boundary experiment on an aqueous sucrose solution. Intergration of the resulting pattern using Simpson's rule yielded a value of 0.1176 cm^2 for the instrument constant relating the deflection from the baseline and the ratio of the refractive index gradient to the tangent of the phase plate angle. The diffusion coefficient determined by the calibration run differed from the hand book value for sucrose by less than 1% indicating that no convection occured during the run. The instrument

TABLE 3

REFRACTIVE INDEX INCREMENTS (ml/g)

	wave length (nm)			
	498.8	568.5	589.3	615.8
DAC	.1564 ± .0013	.1564 ± .0022	.1569 ± .0008	.1571 ± .0009
DMDAC	.1580 ± .0005	.1550 ± .0005	.1539 ± .0007	.1543 ± .0006
TMDAC	.1576 ± .0006	.1546 ± .0007	.1541 ± .0002	.1557 ± .0012

constant along with the required specific refractive index increment was used to obtain the concentration gradients from Schlieren patterns. All runs were performed at 30.0 ±0.2°C.

The procedure used to obtain apparent molecular weights from Archibald data involved extrapolating values of the apparent Archibald variable (i.e. the value of $-(2/\omega^2 d \ln c/dr^2$ or s/D calculated at each radial position as if it were the interface) to the actual interface. A plot of the logarithm of the variable versus displacement was linear in a region close to the interface. The experimental error in these extrapolations was calculated from the slope of the plots multiplied by 0.0025 cm (i.e. the estimated error in the location of the true interface). The concentration at the interface was obtained in a similar way. Appendix A contains the details of a typical analysis.

The details of runs performed on the centrifuge are included in table 4 and the extrapolated intercepts and errors obtained as well as the computed molecular mass are listed with the data in tables 12 through 21.

Viscometry: Non-Newtonian viscosities were determined with a Cannon No. OC A661 capillary viscometer whose

TABLE 4

DETAILS OF RUNS PERFORMED ON THE CENTRIFUGE

RUN		C_o	CMC	$\omega \times 10^{-3}$ (r.p.m.)	$-RT(1-\rho\bar{v})$
1	DAC in .1001 M NaCl	.0227	.0055	30	2.67
2	DAC in .0957 M NaCl	.0267	.0055	20	2.67
3	DAC in .1003 M NaCl	.0346	.0055	20	2.67
4	DAC in .0972 M NaCl	.0423	.0055	20	2.67
5	DAC in .0535 M NaCl	.0420	.0070	20	2.70
6	DAC in .02080 M NaCl	.0298	.0097	60	2.73
7	DAC in .0986 M NaCl and .00076 M NaOH	.0394	.0055	15	2.67
8	DAC in .0994 M NaCl and .00137 M NaOH	.0397	.0055	15	2.67
9	DAC in .0999 M NaCl and .00215 M NaOH	.0399	.0055	10	2.67
10	DMDAC in .0239 M KCl	.0454	.0027	30	2.21
11	DMDAC in .2028 M KCl	.0969	.0027	30	2.21
12	DMDAC in .1027 M KCl	.0989	.0041	36	2.32
13	DMDAC in .0973 M KCl	.2075	.0041	36	2.32
14	DMDAC in .0429 M KCl	.0917	.0065	36	2.37
15	DMDAC in .0439 M KCl	.1153	.0065	36	2.37
16	TMDAC in .0985 M NaCl	.0618	.0072	30	2.64
17	X_{DAC}/X_{TMDAC} = .990 in .0983 M NaCl	.0796	.0062	30	2.64
18	X_{DAC}/X_{TMDAC} = 2.000 in .0988 M NaCl	.0597	.0060	30	2.64

capillary was approximately 9.2 cm in length and 1.98×10^{-2} cm in radius and was modified as shown in figure 3. The viscometer itself was mounted in a bath held at 30.00 ±0.03°C. Flow times of between 0.8000 s and 400.0 s were obtained from an electronic clock capable of accurately resolving 0.001 s. The clock was triggered on and off by the changing output of phototransistors as the solution meniscus passed slits above and below a bulb containing 2.4 ml of solution. Applied pressures of up to 7000 mmHg were obtained by pressurizing a ballast cylinder with nitrogen. The pressure was monitored with a MKS Capacitance Manometer supplied with a digital offset and a 0-10,000 mmHg head. Experimental pressure were corrected for the hydrostatic head due to the liquid column by the "log head" method[61]. Flow times and applied pressures are believed to be accurate to ±0.2%.

Usually, experimental viscosities are found by correcting the applied pressure for the kinetic energy imparted to the fluid at the entrance of the capillary via,

$$\Delta P = P_{applied} - m\rho V^2/\pi^2 R^4 t^2 \qquad (46)$$

where ρ is the solution density, V is the volume of flow, R is the radius of the capillary, t is the time of flow, and m is related to end effects at the exit of the capillary followed by division by the experimental shear rate, G, determined from the volume rate of flow by

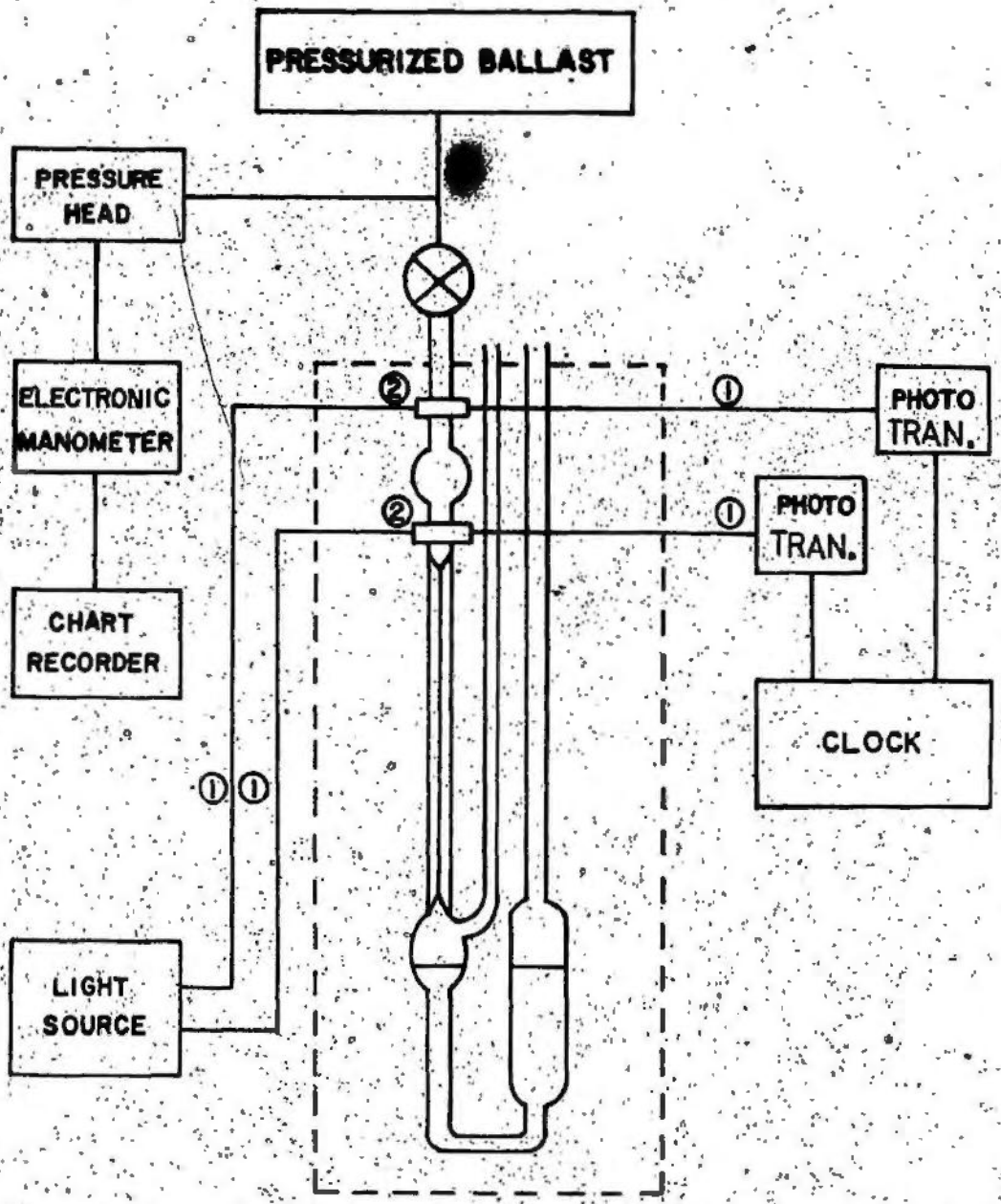

Figure 3 Schematic of viscometer showing fiber optics, (1), and slits, (2).

assuming a parabolic velocity profile[40]. This procedure gave reliable results over most of the range of flow rates used except for the very highest where the value of m changes. An alternative procedure[62] in which the multiplication factor, F, in equation 47 is evaluated at various values of the Reynold's number ($Re = 2V\rho/\pi R\eta t$) during the calibration run on water was useful over the entire range of Reynold's numbers encountered.

$$\eta_{ex} = PtF \tag{47}$$

In this equation P is the applied pressure, t is the flow time and η_{ex} is the experimental viscosity. To apply equation 47 to the non-Newtonian fluids the values of η, Re and F were iterated until a self consistent set was obtained. In order to check this procedure the viscosity of an aqueous solution of 20% sucrose was determined over the entire range of operation of the apparatus and was found to be independent of the shear rate as one would expect.

Experimental viscosities were corrected for non-Newtonian flow by the usual equations[63]. As is always the case when using a Newtonian fluid as a reference standard in relative measurements of viscosity, the viscosities are determined more accurately than the shear rates to which they apply. Uncertainties in apparatus constants (in particular the value of the flow

volume) limit the accuracy of the latter to 4% while the error in the viscosities themselves based on the measurement of flow times and applied pressures are believed to be less than 0.5%. This fact makes corrections to the experimental shear rates unnecessary (i.e. they never exceeded 4%). The corrected viscosities and the value of the Reynold's number and shear rates are listed in tables 22 through 31 along with the pressure corrected for kinetic energy. Reduced specific viscosities defined by,

$$\frac{\eta_{sp}}{c} = \frac{\eta - \eta_{CMC}}{\eta_{CMC} c} \tag{48}$$

where η is the non-Newtonian solution viscosity at a particular shear rate and η_{CMC} is the viscosity at the CMC and c is the concentration of surfactant in excess of the CMC in units of g ml^{-1} were determined using published data for the viscosity of aqueous NaCl solutions[62] and the result of viscosity measurements below the CMC,

$$\eta_{CMC} = \eta_{NaCl} + 2.9CMC \tag{49}$$

where here the CMC is expressed in g ml^{-1} (i.e. a shape factor of 2.9 was used for the monomeric surfactant molecules which are subsequently included as solvent).

RESULTS AND DISCUSSION

Some of the results of centrifugation of DAC are presented graphically in figure 4. Several features of the data are worthy of special note. Firstly, the limiting molecular mass in 0.1 M NaCl varies from a high of about 80,000 g mol^{-1} to a much lower value depending on whether or not the data obtained at concentrations less than 0.015 M is included. The result of the data at higher concentrations compares favourably with the value of 85,500 g mol^{-1} reported by Kushner[5]. It is believed that this steep increase in micellar mass with increasing concentration could easily be overlooked in most investigations. Secondly, the micellar mass is extremely sensitive to small additions of NaOH. The concentrations of NaOH used in these runs represent 6.25%, 4.01% and 2.24% deprotonation of the DAC in the solutions prior to centrifugation. It seems reasonable to assume that the average values of the micellar masses obtained represent DAC micelles whose surface charge has been reduced from its value in 0.1 M NaCl by these percentages. If one assumes a fractional surface charge of 0.23 in 0.1 M NaCl[64], then the average micellar masses of 110,000 g mol^{-1}, 140,000 g mol^{-1} and 210,000 g mol^{-1} correspond to fractional surface charges of 0.21, 0.19 and 0.17 respectively. Thirdly, the concentration dependence of the micellar mass at the two lower salt concentrations is markedly non-ideal,

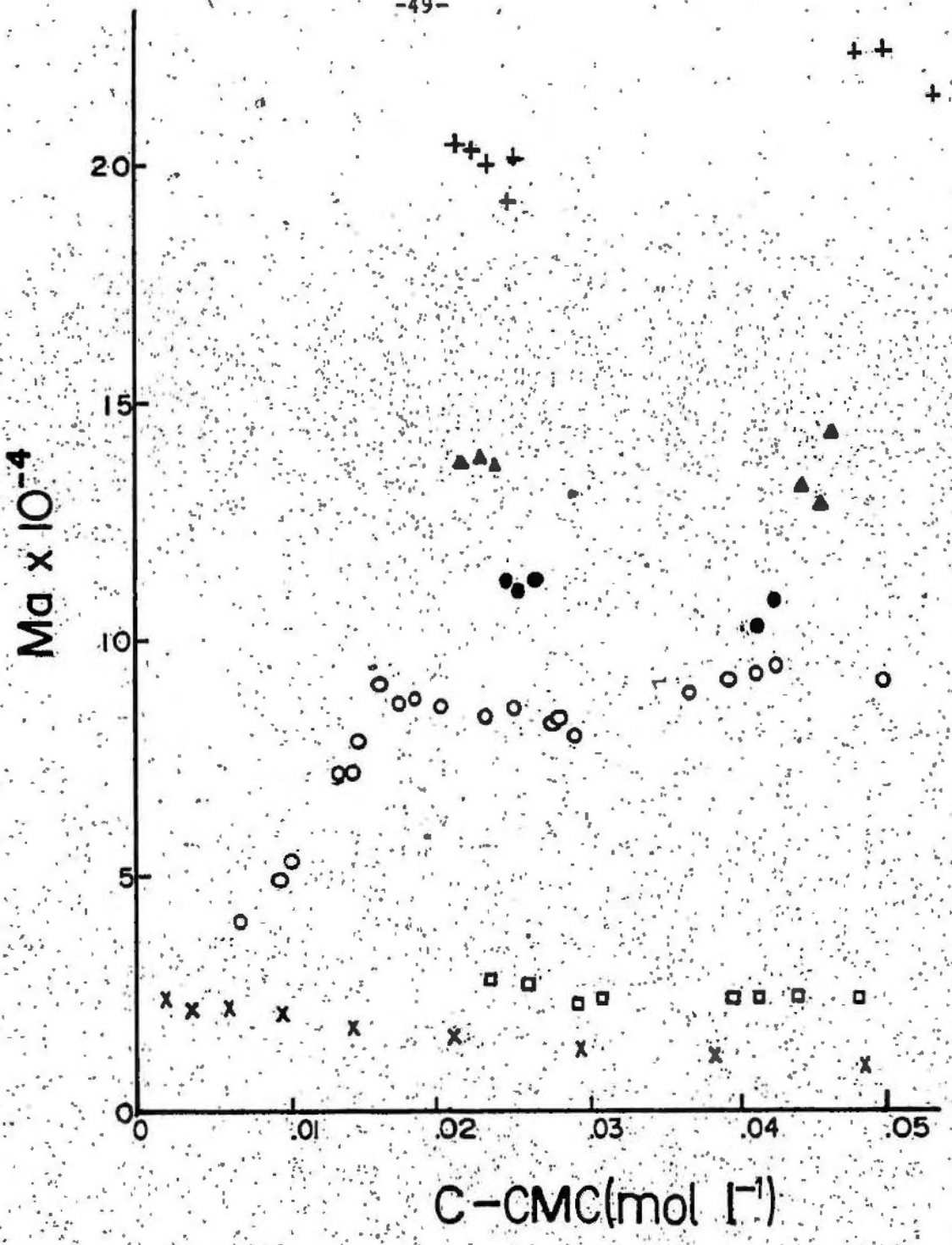

Figure 4 Apparent molecular weights of DAC micelles in 0.1 M NaCl and 0 (o), .00076 (●), .00137 (Δ), .00215 (+) M NaOH and in .054 (□) and .020 (x) M NaCl.

exhibiting a 2.5 fold decrease with increasing surfactant concentration in the case of 0.021 M NaCl. The apparent molar second virial coefficients for equilibrium centrifugation obtained from the slopes and intercepts of the inverse apparent micellar mass versus concentration plots in figure 5 are 30.8 $dm^3\ mol^{-1}$ and 10.3 $dm^3\ mol^{-1}$ for the data in 0.021 M and 0.054 M NaCl respectively. Similar plots of the data obtained for solutions of DMDAC, TMDAC and TMDAC-DAC mixtures are presented in figures 6 and 7 and are also linear suggesting that a second order virial correction which includes the effects of pairwise interactions may be in order. However, it is also possible to interpret this data in terms of the developments included in the theory section, based on a microscopic picture of particle motion, and thereby evaluate the relative importance of the various sources of non-ideal behaviour in these solutions.

In order to complete the analysis a pair interaction potential energy function must be assumed. In view of the analysis by Bell, Levine and McCartney[65] of the approximate methods of determining the double layer free energy of interaction between charged spheres, the familiar form for the interaction energy given by equation 50 was used subject to the condition that the effective charge parameter was allowed to vary so as to produce the best possible fit to the data. Hence, i takes the value which produces

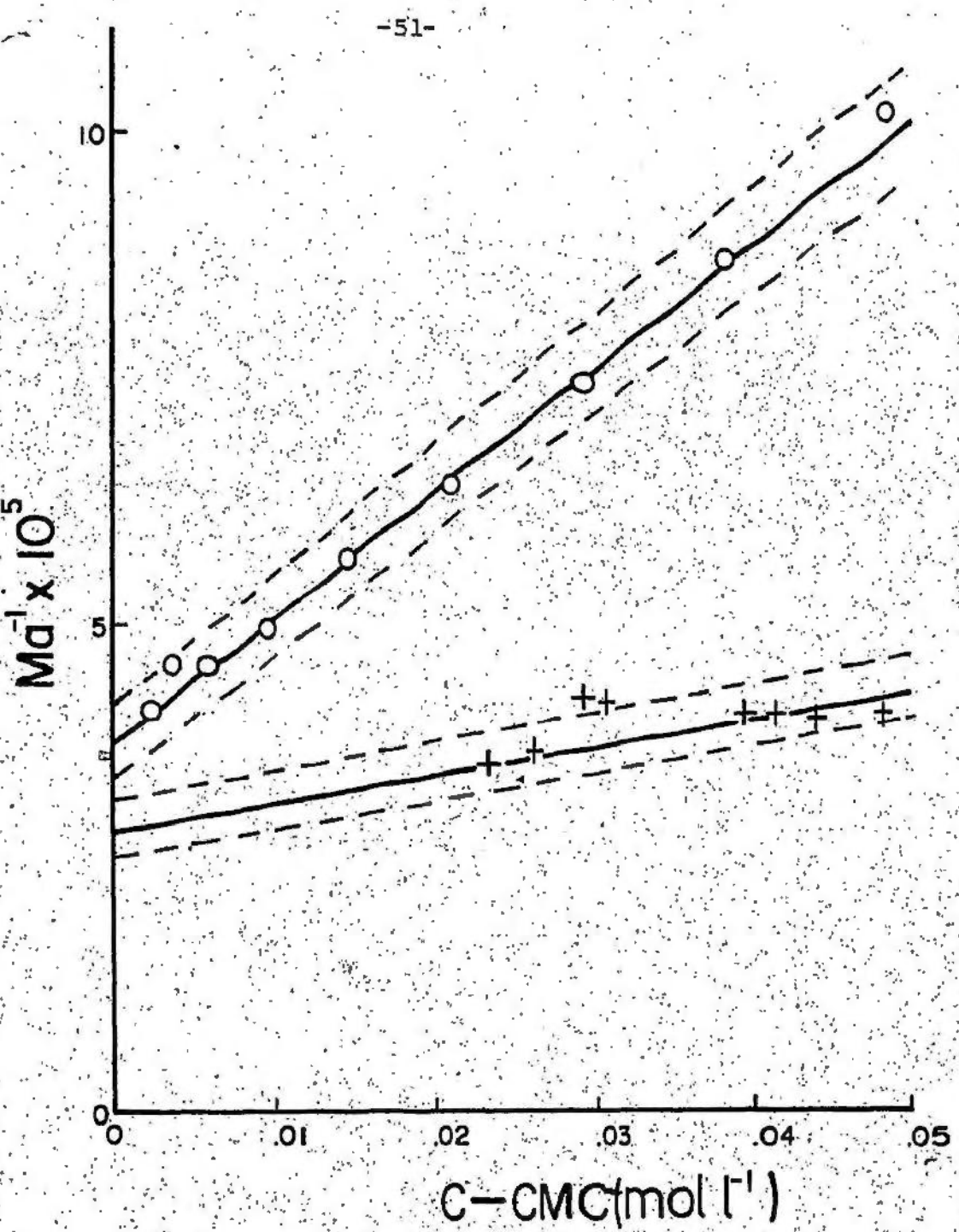

Figure 5 Concentration dependence of inverse apparent micellar molecular weight of DAC in .054 (+) and .021 (o) M NaCl. Solid curves are from equation 32 with parameters from table 5 . Dashed curves are computed by assuming ±10% error in z.

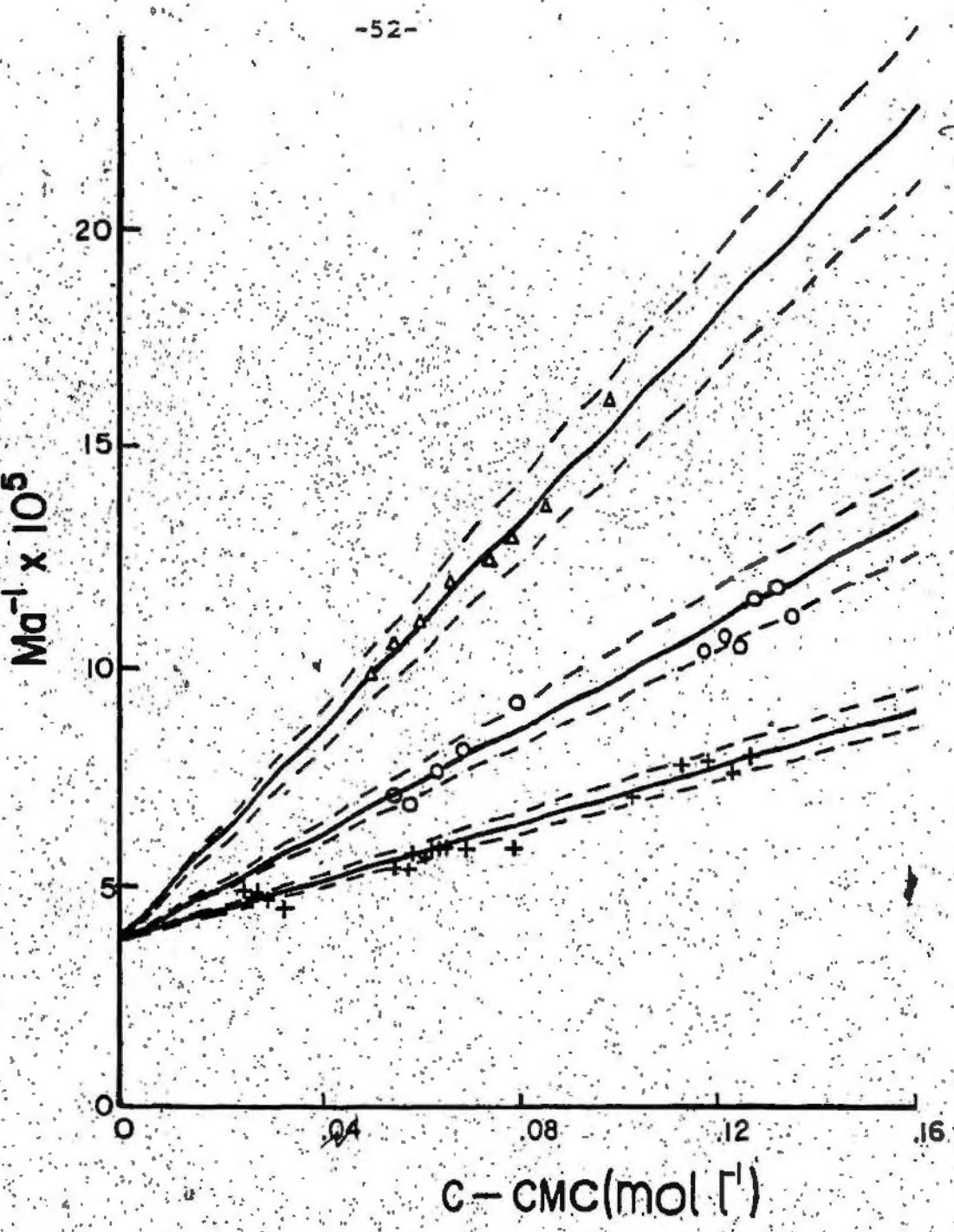

Figure 6. Concentration dependance of inverse apparent micellar molecular weight of DMDAC in .20 (+), .10 (o) and .043 (Δ) M KCl. Solid curves are from equation 32 with parameters from table 5. Dashed curves are computed by assuming ± .01 error in i.

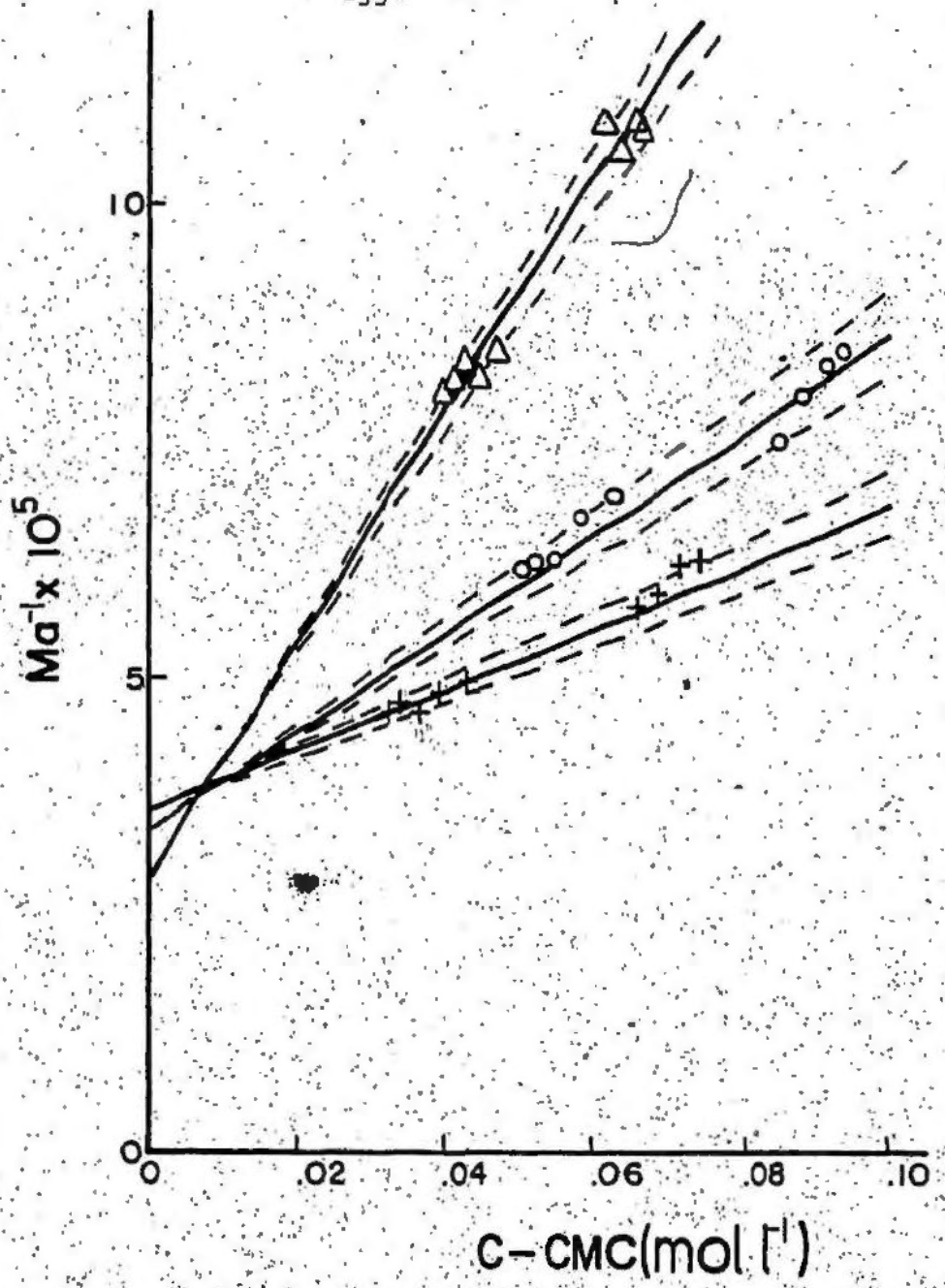

Figure 7 Concentration dependence of inverse apparent micellar molecular weight of TMDAC (Δ), $X_{DAC}/X_{TMDAC} = 1$ (o) and $X_{DAC}/X_{TMDAC} = 2$ (+) in .10 M NaCl. Solid curves are from equation 32 with parameters from table 5 . Dashed curves are obtained by assuming $\pm 3 \times 10^{-8}$ cm error in a.

the best representation of the interaction energy in the region over which most of the pair interactions resulting in non-ideal behaviour occur.

$$W/k_BT = \frac{(ize)^2 \exp(-2\kappa a\rho)}{2\varepsilon a\, k_BT(1+\rho)} \qquad (50)$$

In equation 50 ρ is the reduced interparticle separation, ε is the dielectric constant (assumed to be 76.6), a is the radius of the hydrodynamic particle and κ is the Debye parameter defined by,

$$\kappa = (8\pi e^2 NI/\varepsilon k_BT) \qquad (51)$$

where e is the electronic charge and I is the ionic strength calculated by adding the CMC to the concentration of simple salt.

The results of fitting the apparent inverse micellar mass to equation 18 by using equation 50 to numerically integrate the expressions in equations 19 and 20 and identifying c_p with (c-CMC)/z are listed in table 5. In this table k_1 and k_2 refer to the molar second virial coefficients of mutual and tracer diffusion defined by equation 18 and the hydrodynamic specific volume, $\bar{v}_h$,

$$k_1 = 8(I-\Lambda)M_m\bar{v}_h/1000 \qquad (52)$$

$$k_2 = 8\Lambda M_m\bar{v}_h/1000 \qquad (53)$$

where M_m is the anhydrous mass of the surfactant monomer and $\bar{v}_h$ is given in terms of the hydrodynamic radius and the aggregation number by,

$$\bar{v}_h = 4\pi a^3 N/3zM_m \qquad (54)$$

TABLE 5

PARAMETERS AND RELATED VALUES DERIVED FROM THE FIT OF CENTRIFUGE DATA TO EQUATION 32

	z	i	$-(1-\bar{p}\bar{v})$	k_1 (dm^3/mol)	k_2 (dm^3/mol)	$i(1+\kappa a)$
DAC in .021 M NaCl	110	.085	.092	15.0	.61	.22
DMDAC in .043 M KCl	95	.135	.106	14.5	.52	.40
DMDAC in .10 M KCl	95	.120	.109	7.8	.59	.45
DMDAC in .20 M KCl	95	.110	.114	4.4	.65	.54
TMDAC in .10 M NaCl	110	.235	.095	12.9	.46	.89
$X_{DAC}/X_{TMDAC} = 1$ in .10 M NaCl	110	.115	.094	7.6	.53	.44
$X_{DAC}/X_{TMDAC} = 2$ in .10 M NaCl	110	.075	.094	5.1	.58	.29
DAC in .054 M NaCl	150	.050	.098	5.6	.73	.18

Since the reduced specific viscosity of DMDAC showed no non-Newtonian behaviour but was approximately 2.5 times greater than the intrinsic value for spheres[9], a value of 2.5 ml g^{-1} was assumed for $\bar{v}_h$ allowing a to be calculated from z via equation 54. Fortunately, the results of the analysis did not vary much with the value of a input as shown in figure 7 so that the error introduced by this approximation is small. Hence, the input values of only z and i completely determine all aspects of the fit within a data set, assuming constant aggregation numbers. The best fit, shown as a solid curve in the figures, was obtained by varying the values of z and i by increments of 5 and 0.005 respectively until the deviations of the points from the curve was minimized. The graphic analysis was performed on a Tektronics 4051 with numerical integrations computed in a PDP 1170. The dependence of the fit on the values of z and i is substantial as shown in the figures.

The goodness of the fits is remarkable in that not only are they obtained by assuming constant aggregation number within a data set but also because the best aggregation number obtained for all sets was relatively constant except for the case of DAC in 0.055 M NaCl. This result suggests that at least some of the variation in aggregation number reported[5,6] for TMDAC micelles may be due to the lack of correction for non-ideality.

Using Henry's first order correction for the charge

on a colloidal particle to estimate the fractional surface charge from the effective charge parameter,

$$\text{fractional surface charge} = i(1 + \kappa a) \qquad (55)$$

results in the values included in the last column of table 5. An interesting plot showing the variation of aggregation number with this surface charge and including the values for deprotonated DAC solutions is shown in figure 8. The plot shows that aggregation in this group of surfactants primarily depends on the surface charge and on the identity of the head group or groups and the addition of base only in as much as these latter factors influence the former. The results also show that the charge obtained in mixed micelle solutions is not a weighted linear combination of the individual value, but is in fact much less. This seems in accordance with the non-linear way in which the CMC varies with mole fraction in mixed micellar solutions[66] and indicates that more favourable packing arrangements are possible in mixed micelles.

Reduced specific viscosities obtained via equation 48 of several solutions containing large DAC micelles are plotted in figures 9 through 12 as a function of the shear rate to which they apply. As expected, all solutions exhibit non-Newtonian behaviour in accordance with the theories[42,67,68] for the alignment of anisotropic particles at high rates of shear in that the viscosity eventually drops as the shear rate increases. However,

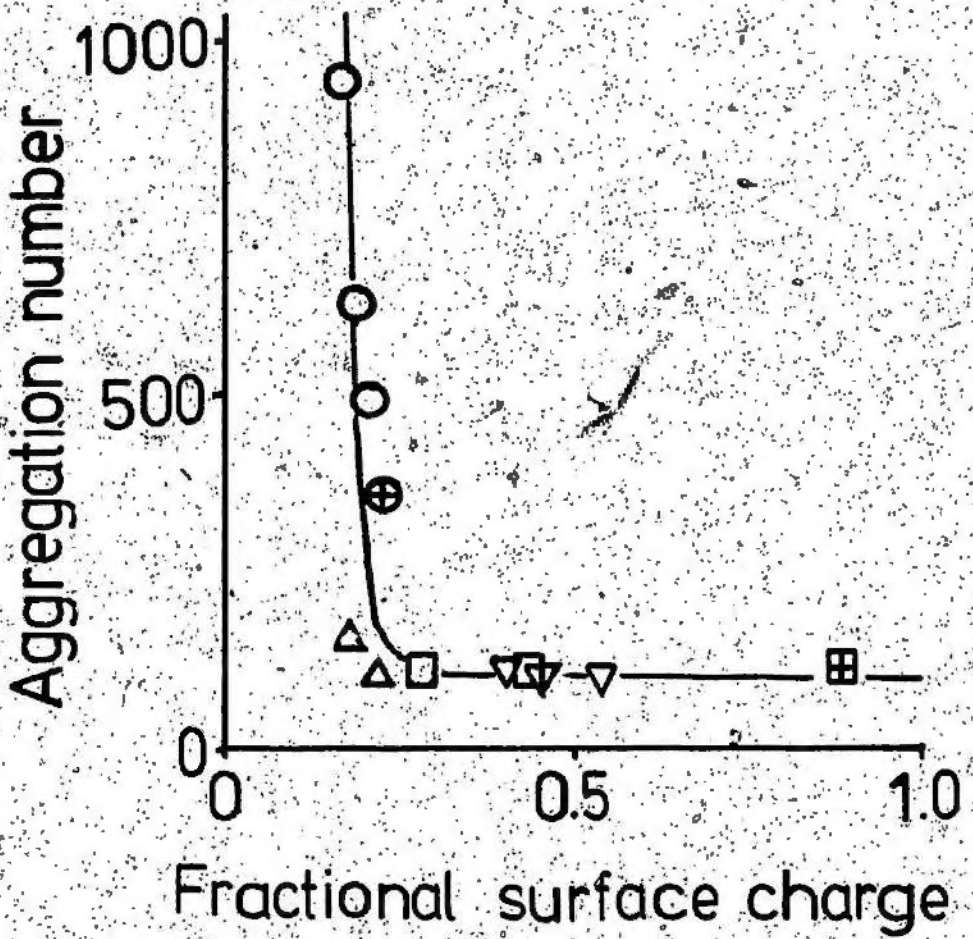

Figure 8 Trend in aggregation of dodecylammonium salts with surface charge. Deprotonated DAC (○) and DAC (⊕) in 0.1M NaCl (see reference 64). DAC (△) in 0.054 M NaCl and 0.021 M NaCl. DMDAC (▽) in 0.043 M, 0.10 M and 0.20 M KCl. TMDAC-DAC mixtures (□) and TMDAC (⊞) in 0.10 M NaCl.

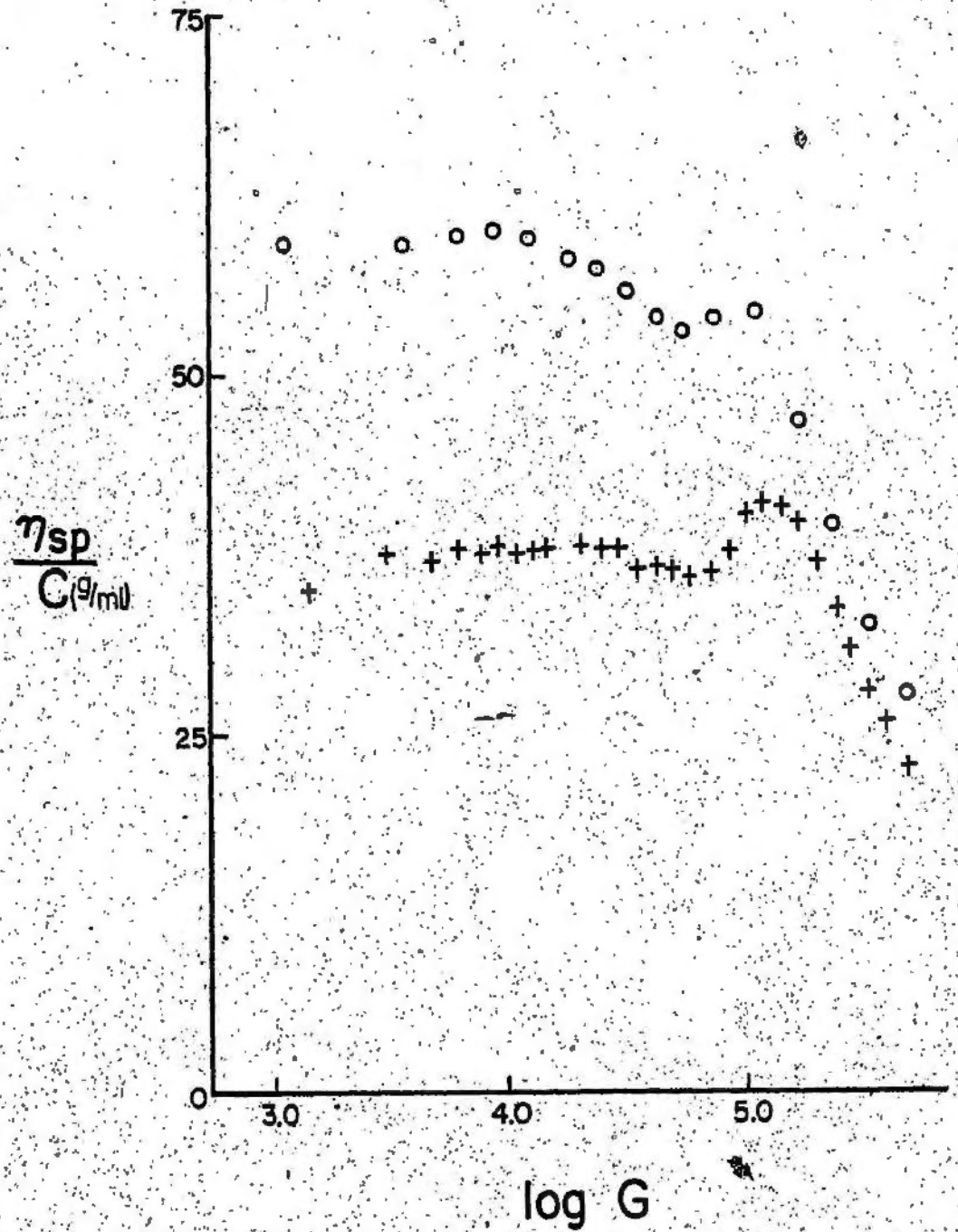

Figure 9. Shear dependence of viscosity of .01798 (+) and .03639 (o) M DAC in .20 M NaCl.

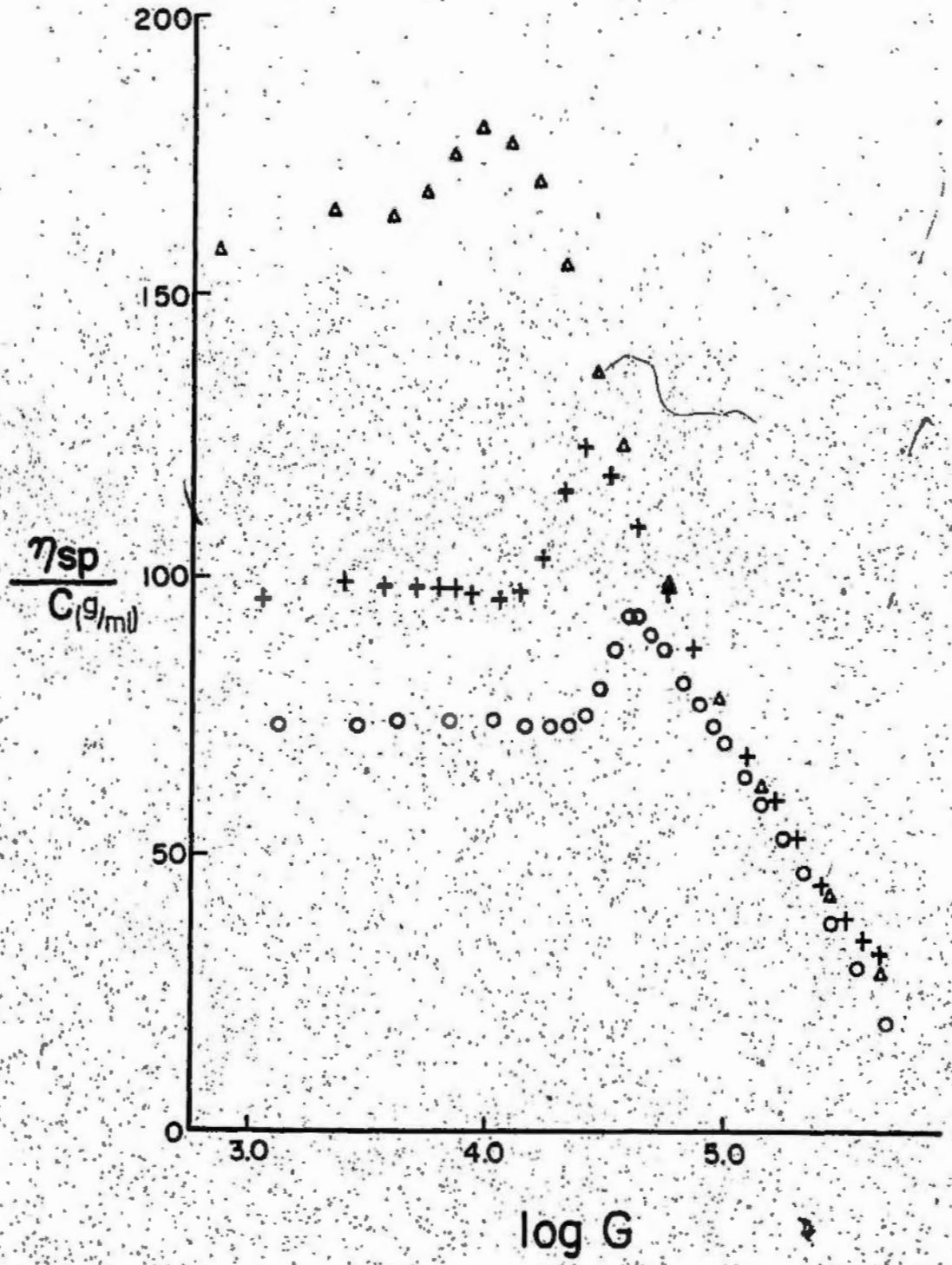

Figure 10 Shear dependence of viscosity of .01725 (o), .02256 (+) and .03577 (Δ) M DAC in .25 M NaCl.

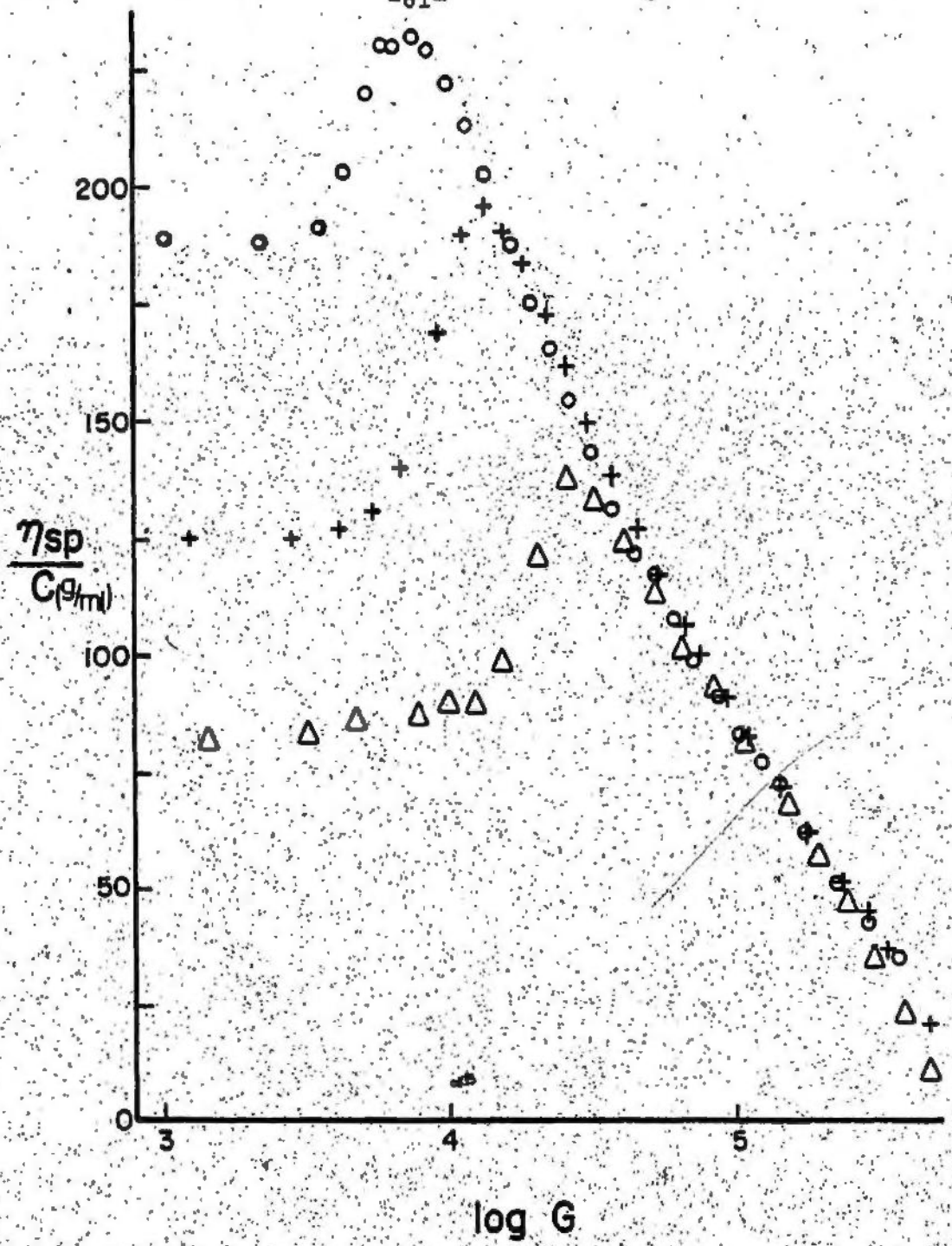

Figure 11. Shear dependence of viscosity of .01815 (o), .01363 (+) and .00907 (Δ) M DAC in .30 M NaCl.

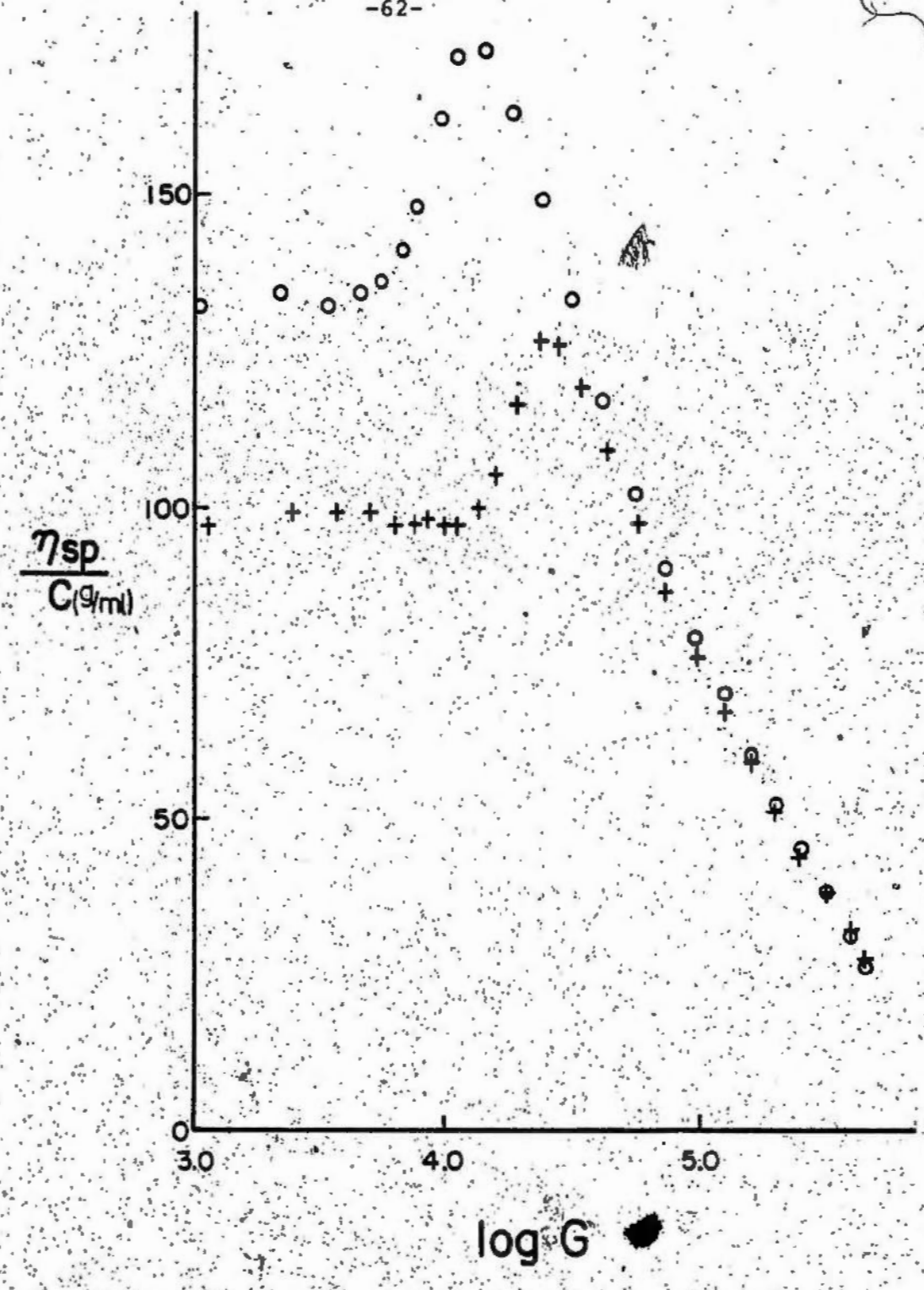

Figure 12. Shear dependence of viscosity of .02257 M DAC in .1516 M NaCl and .0996 M HCl (+), and .02263 M DAC in .2509 M NaCl and .000390 M NaOH (o).

these theories do not predict or account for the experimentally observed region in which the viscosity increases with increasing shear rate which was found in all solutions. That this phenomena was not just an experimental artifact due to thixotropy or instability was deduced from the independence of the results on different experimental procedures including passing the same sample through the viscometer several times in succession and collecting data by increasing the shear rate as well as by decreasing it. Furthermore, the viscosity of a sucrose solution more viscous than any surfactant solution was obtained without any anomalies over the entire range of shear rates studied. Finally, the anomalous region almost always was found to occur at Reynolds numbers less than those normally associated with turbulent flow and in fact the results of turbulent flow observed in preliminary work on more viscous solutions was qualitatively different in that the value of the apparent viscosity increased much more rapidly and apparently without limit. Therefore, it is believed that the data obtained is real and representative of some feature of the hydromechanics of these solutions in capillary viscometers which is not as yet understood.

This anomalous feature might conceivably arise from one of the following sources:

(1) A shear dependence of the CMC which would effectively increase the volume of micelle at high shear rates.

This could be a result of increased collision frequency at high shear rates. A comparison of the CMC's and total concentrations employed indicates that a 30% increase is possible in some solutions. However, there is no systematic relationship between CMC/c and the magnitude of the increase which would support this explanation.

(2) Redistribution of micellar size in the shear field. In this case one might expect the effect to increase with increasing surfactant concentration but although the reduced specific viscosity did increase the increase in the anomalous region was largely unaffected.

(3) Inadequacies in the theories for the effects of flexibility or entanglement. These effects have often been cited when experimental results would not otherwise coincide with theory[44,46,69,70].

(4) Special flow instabilities which are unique to these solutions. The lack of theoretical developments to explain the early recognized anomalous behaviour of dilute colloidal solutions in unusual flows[71] has been recently noted as a major shortcoming in the general development of micelle theory[72]. The results of the present study confirm that this is indeed true and cast doubt on the validity of analysis of rheological data on these systems including that obtained even at low shear rates.

One can, however, make some qualitative comments on general features of the results. Firstly, in the presence

of sufficient simple salt, DAC micelles are certainly large and anisotropic. Comparison of the rate at which the reduced specific viscosity decreases with increasing shear rate with the numerical results of Scheraga[43] for rigid ellipsoids suggests that the micelles behave more like prolate than oblate ellipsoids. Finally, the viscosity, like the centrifuge results, is very sensitive to the addition of NaOH, but is insensitive to the addition of HCl as can be seen from a comparison of the curves in figure 11 with the corresponding run in figure 9 done at the same ionic strength.

In conclusion, it is important to assess, at least qualitatively, the advantages and limitations of the methods employed in this study and to identify the areas of micellar research which would be well served by an extension of these preliminary results. Firstly, quite apart from the microscopic analysis of the concentration dependence, centrifugation is intrinsicly a thermodynamic method. That is, the micellar molecular wieghts obtained from extrapolation of results to the CMC are independent of any assumptions concerning micelle structure or behavior. In contrast, all so called "dynamic" methods, which are currently popular, depend for their analysis on assumptions about shape, hydration and ionization of the micelle. Although it is quite likely that these cause little error in systems containing small micelles, it is not at all clear

that the experimentally determined "effective spherical radius" can be simply related to micellar dimensions when larger micelles are suspected. It is interesting to observe that Mazer[10] et. al. have attributed the increase in effective radius obtained from quasielastic light scattering of sodium dodecylsulfate solutions to micellar growth while Corti and Degiorgio[73] interpret similiar data in terms of attractive interactions via DVLO[74] theory.

Unfortunately, it is rarely possible to obtain reliable data at sufficiently low concentrations for the limiting value of the micellar mass to be accurately determined. Hence, observation of the proposed "minimum sphere" micelle[75] at concentrations just greater than the CMC has often proved impossible. In this respect, ultracentrifugation is more flexable than many techniques in that the initial solution concentration, speed and duration of the run as well as expansion of the refractive index gradients by adjustment of the phase plate can be chosen to optimize evaluation of the parameters. As an example, the growth region exibited by DAC in 0.1 M NaCl, illustrated in figure 4 was completely overlooked in the original examination of this system by the method of clasical light scattering[5].

It is in the analysis of the concentration dependence, however, that the most interesting characteristics of these micellar solutions becomes apparent. Recently, a

classification scheme has been proposed by Dorshow[76] et. al. to separate their dynamic light scattering data on cetyltrimethylammonium bromide (CTAB) into three regions for the purposes of theoretical analysis. They include a region at high ionic strengths in which the apparent diffusion coefficient decreases with increasing surfactant concentration, a transition region and a region at low ionic strength in which the apparent diffusion coefficient increases with increasing surfactant concentration. This scheme is equally applicable to the systems studied herein. Since it is obvious that the behavior can vary in both type and degree, it is not surprising that the analysis developed in the theory section is not applicable in all circumstances. Therefore, this work limits itself (as did Dorshow's) to the detailed analysis of the latter region only simply because the required interaction potentials for the other two regions are not avaible. With this limitation, however, the theory for the analysis of centrifuge data on micellar solutions in terms of measurable ancillary quantities has been developed in terms of a relatively small number of adjustable parameters. The most interesting of these is the effective charge prameter which can be determined quite precisely and which exibits a critical value, above which large micelles do not form. The extent of aggregation in this region is insensitive to

increasing surfactant concentration and ionic strength. The optimum aggregation numbers reported in table 5 were obtained by a searching proceedure using increments of 5 in the value of z. Since the dependence of the fits is rather sensitive to z, it is likely less than about two increments or ±10. Neglecting the value of 150 for DAC in 0.054 M NaCl (to be discused presently) leads to an average value of 100±10. Essentially identical conclusions involving a higher constant value of z have been adopted by Dorshow's group. They also find that micellar charge can be precisely determined in a modern analysis of non-ideal behavior.

Since this group finds it necessary to include an attractive potential term in their analysis of partical interaction, at least in weakly non-ideal systems, it is important to evaluate the error incured from omission of this term in the present work. Qualitatively, one would expect that as the interaction potential becomes increasingly more attractive the optimum value of the micelle charge required to produce a fit, maintaining constant z and r, would decrease below it's true value to compensate for neglecting these interactions. In the rus on DMDAC, however, it was found that $i(1+\kappa a)$ actually increases with increasing ionic strength so that neglecting this term is justified. For DAC micelles,which have lower fractional surface charge, the opposite trend was observed. Therefore, the value of 150

obtained in 0.054 M NaCl maybe somewhat of an overestimation. It should be noted here that the charge parameter adjusted by Henry's correction is an approximation to the actual surface charge which would be slightly larger if further corrections were applied or an exact computer calculation of the repulsive potential adopted.

Lastly, an interesting suggestion by Dorshow that micellar growth may occur as a result of coalescence of small micelles when the attractive contribution to the interaction potential becomes dominant requires some comment. This rather subtle suggestion would require as a corollary that all solutions of small micelles are intrinsicly non-ideal. This simple fact appears credible considering the on-going controversy which has surrounded evaluation of the most basic micellar parameter, the micellar mass. Also, if correct, then molecular wieght distributions would be expected to be affected by any perturbation of micelle collision frequency such as that which occurs under shearing conditions in the viscometer. Therefore, the development of a theoretical framework in which variable shear viscometry could be analysed (particularly the anomalous region) may help shed valuable light on some fundamental aspects of micelle dynamics. This, however, is outside the scope of the present investigation.

NOTES AND REFERENCES

(1) McBain, J.W. *Trans. Faraday Soc.* 9, 99 (1913).

(2) Hartley, G.S. "Aqueous Solutions of Paraffin Chain Salts" Hermann, Paris, 1936.

(3) Tanford, C. "The Hydrophobic Effect" 2nd Ed., Wiley, New York, 1980.

(4) Greer, R.D.; Eylar, E.H. and Anacker, E.W. *J. Phys. Chem.* 75, 369 (1971).

(5) Kushner, L.M.; Hubbard, W.D. and Parker, R.A. *J. Res. Nat'l. Bur. Stand.* 59, 113 (1957).

(6) Emmerson, M.F. and Holtzer, A. *J. Phys. Chem.* 71, 1898 (1967).

(7) Adair, D.A.W.; Reinsborough, V.C.; Plavac, N. and Valleau, J.P. *Can. J. Chem.*, 52, 429 (1974).

(8) Attwood, D. *J. Phys. Chem.* 72, 339 (1968).

(9) Einstein, A. *Ann. Phys. Lpz.* 19, 289 (1906).

(10) Mazer, N.A.; Benedek, G.B. and Carey, M.C. *J. Phys. Chem.* 80, 1075 (1976).

(11) Svedberg, T. and Pedersen, K.O. "The Ultracentrifuge" Oxford University Press, Oxford, 1940.

(12) Schachman, H.K. "Ultracentrifugation in Biochemistry" Academic Press, New York, 1959.

(13) Tanford, C. "Physical Chemistry of Macromolecules" Wiley, New York, 1969.

(14) Kratohvil, J.P. *J. Colloid and Interface Sci.* 75, 271 (1980).

(15) Doughty, D.A. *J. Phys. Chem.* 20, 2621 (1979).

(16) Fisher, L.R. and Oakenfull, D.G. *Chem. Soc. Rev.* 6, 25 (1977).

(17) Fujita, H. "Foundations of Ultracentrifugal Analysis", Chemical Analysis, Vol. 42, Wiley, New York, 1975.

(18) Einstein, A. *Ann. Physik* 17, 549 (1905).

(19) Chervenka, C.H. "A Manual of Methods for the Analytical Ultracentrifuge" Spinco Division of Beckman Instruments, California, 1973.

(20) Peacocke, A.R. and Schachman, H.K. *Biochem. et Biophys. Acta* 15, 198 (1954).

(21) Boedtker, H. and Simmons, N.S. J. Am.Chem. Soc. 80, 2550 (1958).

(22) Crank, J. "The Mathematics of Diffusion" Oxford University Press, Oxford, 1956.

(23) Archibald, W. J. J. Phys. Chem. 51, 1204 (1947).

(24) Yphantis, D. A. *Biochemistry* 3, 297 (1964).

(25) Johnson, S.J.; Kraus, K.A. and Scatchard, G. J. Phys. Chem. 58, 1034 (1954).

(26) Fujita, H., Inagaki, H., Kotaka, T. and Utiyama, H. J. Phys. Chem. 66, 4 (1962) 66, 4 (1962).

(27) Aniansson, E. A. G. and Wall, S. N. J. Phys. Chem. 78, 1024 (1974).

(28) Eisenberg, H. *Biophysical Chemistry*, 5, 243 (1976).

(29) Pedersen, K. O. J. Phys. Chem. 62, 1282 (1958).

(30) Arfken, G. "Mathematical Methods for Physicists" Academic Press, New York, 1970.

(31) Anacker, E. W.; Rush, R. M. and Johnson, J. S. J. Phys. Chem. 68, 81 (1964).

(32) Alexandrowicz, Z. and Daniel, E. *Biopolymers* 1, 447 (1963).

(33) Alexandrowicz, Z. and Daniel, E. *Biopolymers* 1, 473 (1963).

(34) Mijnlieff, P. F. in "Ultracentrifugal Analysis", Williams, J. W. Ed.; Academic Press, New York, 1963.

(35) Varoqui, R. and Schmitt, A. *Biopolymers* 11, 1119 (1972).

(36) Lamm, O. *Arkiv Kemi, Mineral., Geol.* 17A, No.25 (1944).

(37) See reference 38.

(38) A complete bibliography of the early theoretical and experimental work is given in: Tolman, R. C. *J. Am. Chem. Soc.* 33, 121 (1911).

(39) Mukerjee, P. and Mysels, K. J. "Critical Micelle Concentrations of Aqueous Surfactant Systems" NSRDS-NBS-36, Superintendent of Documents, U.S. Government Printing Office, Washington, D.C. 20402, 1971.

(40) Stokes, R. H. and Mills, R. "Viscosity of Electrolytes and Related Properties" Vol.3 in "The International Encyclopedia of Physical Chemistry and Chemical Physics" Guggenheim, E. A.; Mayer, J. E. and Tompkins, F. C,, Ed., Pergamon Press, Oxford, 1965.

(41) Frisch, H. L. and Simha, R. in "Rheology" Vol.I; Eirich, F. R., Ed.; Academic Press, New York, 1956, Chapter 14.

(42) Saito, N. *J. Phys. Soc. Japan* 6, 297 (1951).

(43) Scheraga, H. A. *J. Chem. Phys.* 23, 1526 (1955).

(44) Layee, Y. and Wolff, C. *J. Polymer Sci.* 11, 1653 (1973).

(45) Booth, F. *Proc. Roy. Soc. (London)* A203, 533 (1950).

(46) Stigter, D. *J. Phys. Chem.* 70, 1323 (1966).

(47) Peterlin, A. *J. Polymer Sci.* 8, 173 (1952).

(48) Anderson, J. L. and Reed, C. O. *J. Phys. Chem.* 64, 3240 (1976).

(49) Rushton, E. and Davies, G. A. *Appl. Sci. Res.* 28, 37 (1973).

(50) Batchelor, G. K. *J. Fluid Mech.* 52, 245 (1972).

(51) Hill, T. L. "An Introduction to Statistical Thermodynamics" Addison-Wesley, Reading, M.A., 1960, Chapter 19.

(52) Casassa, E. F. and Eisenberg, H. *Advan. Protein. Chem.* 19, 287 (1964), see page 360.

(53) The surface tension of pure water was taken to be 71.2 dynes cm^{-1}.

(54) Adamson, A. W. "The Physical Chemistry of Surfaces" Interscience, New York, 1960.

(55) Wentworth, W. E. *J. Chem. Ed.* 42, 96 (1965).

(56) See reference 39 for the pertinent data.

(57) Harned, H. S. and Owen, B. B. "The Physical Chemistry of Electrolytic Solutions" 3rd edition, Reinhold, New York, 1958, pg. 358.

(58) Baxter, G. P. and Wallace, C. C. *J. Am. Chem. Soc.* 38, 70 (1916).

(59) See for example: Hutchinson, E. and Mosher, C. S. *J. Colloid Sci.* 11, 352 (1956).

(60) "Smithsonian Physical Tables" 1954, Table 551.

(61) Barr, G. *J. Chem. Soc, London* 1793 (1935).

(62) Swindells, J. F.; Hardy, R. C. and Cottington, R. L. *J. Natl. Bur. Stds.* 52, 105 (1954).

(63) Yang, J. T. *J. Am. Chem. Soc.* 80, 1783 (1958).

(64) Ralph, E. K. and MacNeil, J. M. Unpublished. The quoted result was obtained by electrochemically measuring chloride concentration in DAC solutions containing varying amounts of NaCl using Cl^-/AgCl half cells.

(65) Bell, G. M.; Levine, S. and McCartney, L.N. *J. Colloid and Interface Sci.* 33, 335 (1970).

(66) Rubingh, D. N. in "Solution Chemistry of Surfactants" Mittal, K. L., Ed., Plenum Press, New York, 1979.

(67) Kuhn, W. and Kuhn, M. *Helv. Chem. Acta* 28, 97 (1945).

(68) Riseman, J. and Kirkwood, J. G. *J. Chem. Phys.* 18, 512 (1950).

(69) Peter, S. *Kolloid Z.* 114, 44 (1949).

(70) Van Oene, H. and Cragg, L. H. *J. Poly. Sci.* 57, 209 (1962).

(71) Hartley, G. S. *Nature* 142, 161 (1938).

(72) Hartley, G. S. in "Micellization, Solubilization and Microemulsions" Mittal, K. L., Ed., Plenum Press, New York, 1977, page 23.

(73) Corti, M. and Degiorgio, V. J. J. Phys. Chem. 85, 711 (1981).

(74) Verwey, E. J. and Overbeek, J. G. T. "Theory of the Stability of Lyophobic Colloids" Elsevier, New York, 1948.

(75) Dorshow, R.; Briggs, J.; Bunton, C. A. and Nicoli, D. F. J. Phys. Chem. 86, 2388 (1982).

(76) Stigter, D. and Hill, T. L. J. Phys. Chem. 63, 551 (1959).

DATA

TABLE 6

SURFACE TENSION OF SOLUTIONS CONTAINING DMDAC AND KCl

[KCl] = 0		[KCl] = 0.393		[KCl] = .1429	
C_{DMDAC}	γ (dyne/cm)	C_{DMDAC}	γ (dyne/cm)	C_{DMDAC}	γ (dyne/cm)
0	71.2	0	71.6	0	71.6
.00186	61.7	.000296	60.9	.000126	61.3
.00335	55.3	.000591	57.0	.000252	56.6
.00495	51.1	.000885	53.6	.000378	53.7
.00704	47.2	.00118	51.9	.000502	51.9
.00832	44.3	.00147	49.9	.000627	49.6
.0105	41.8	.00176	48.7	.000788	47.6
.0118	40.2	.00205	47.2	.00100	46.1
.0138	38.7	.00234	46.0	.00125	44.7
.0167	38.1	.00264	45.0	.00150	42.1
.0195	38.7	.00284	44.8	.00179	41.5
.0225	38.9	.00327	43.3	.00211	39.8
.0252	38.7	.00362	42.3	.00244	38.1
.0278	38.7	.00404	41.8	.00285	36.6
		.00446	40.6	.00325	35.6
		.00495	39.6	.00374	35.6
		.00560	38.7	.00433	35.6
		.00666	37.2	.00504	35.6
		.00800	37.0		
		.0112	37.0		
		.143	37.1		

TABLE 7

DENSITIES OF SOLUTIONS OF DAC CONTAINING 0.1010 m NaCl AT 30.00°C

m	E (mm)	ρ (g/ml)	$(\rho-\rho_{calc})^* \times 10^5$
.01351	60.703	.999548	-.0
.02256	60.997	.999364	.1
.03157	61.297	.999175	-.2
.04058	61.587	.998992	.2
.04963	61.893	.998799	-.1

*Calculated using equation 42 with parameters from table 2.

TABLE 8

DENSITIES OF SOLUTIONS OF DMDAC CONTAINING 0.1002 m NaCl AT 30.00°C

m	E(mm)	ρ(g/ml)	$(\rho-\rho_{calc})^{*} \times 10^{5}$
.00998	60.767	.999509	-.7
.02996	61.543	.999019	1.8
.04995	62.400	.998480	-1.1
.06992	63.177	.997992	.6
.08913	63.970	.997492	-1.2
.10974	64.757	.996998	.8

*Calculated using equation 42 with parameters from table 2.

TABLE 9

DENSITIES OF SOLUTIONS OF TMDAC CONTAINING 0.0996 m NaCl AT 30.00°C

m	E(mm)	ρ(g/ml)	$(\rho-\rho_{calc})^{*} \times 10^{5}$
.00858	60.757	.999515	.2
.02075	61.500	.999047	-.3
.04449	62.203	.998604	-.3
.06237	62.887	.998174	.7
.08143	63.640	.997700	-.3

*Calculated using equation 42 with parameters from table 2.

TABLE 10

DENSITIES OF SOLUTIONS OF DAC AND TMDAC (X_{DAC}/X_{TMDAC} = .924) CONTAINING 0.1003 m NaCl AT 30.00°C

m	E(mm)	ρ(g/ml)	$(\rho-\rho_{calc})^* \times 10^5$
.00905	60.723	.999536	-.6
.02730	61.357	.999137	.1
.04614	61.983	.998742	1.7
.06625	62.700	.998292	.2
.10516	64.053	.997440	-2.2
.14842	65.440	.996567	1.0

*Calculated using equation 42 with parameters from table 2.

TABLE 11

REFRACTIVE INDEX DATA AT 20.00°C

		wave length (nm)			
	c(g/ml)	498.8	568.5	589.3	615.8
H_2O		1.33645	1.33364	1.33299	1.33225
DAC	.00541	1.33743	1.33459	1.33389	1.33313
"	.01099	1.33828	1.33542	1.33475	1.33399
"	.01585	1.33905	1.33619	1.33552	1.33477
"	.02180	1.33999	1.33715	1.33646	1.33570
DMDAC	.01621	1.33903	1.33619	1.33554	1.33477
"	.03094	1.34136	1.33849	1.33780	1.33703
"	.04703	1.34392	1.34100	1.34031	1.33955
"	.06282	1.34639	1.34341	1.34270	1.34195
TMDAC	.01216	1.33836	1.33557	1.33492	1.33410
"	.02482	1.34039	1.33756	1.33687	1.33612
"	.03755	1.34238	1.33949	1.33883	1.33804
"	.05069	1.34444	1.34154	1.34086	1.34012

TABLE 12

ULTRACENTRIFUGE DATA FOR SOLUTIONS CONTAINING DAC AND .1 M NaCl

RUN	t (min)	C-CMC	σ_c	$\overline{-S/D} \times 10^7$	$\sigma_{S/D} \times 10^7$	$Ma \times 10^{-3}$
1	122	.0069	.0002	1.46	.02	40.0
1	74	.0093	.0002	1.78	.05	47.5
1	66	.0101	.0003	1.93	.08	51.6
2	86	.0135	.0002	2.59	.06	69.2
2	70	.0143	.0002	2.60	.06	69.5
2	54	.0148	.0002	2.83	.08	75.6
3	80	.0161	.0003	3.27	.09	87.4
3	64	.0173	.0003	3.12	.09	83.3
3	48	.0186	.0003	3.16	.10	84.4
3	32	.0204	.0004	3.11	.11	83.0
4	57	.0231	.0004	3.02	.09	80.7
4	40	.0252	.0005	3.09	.12	82.5
2	70	.0276	.0004	2.97	.13	79.3
4	24	.0278	.0005	3.01	.13	80.1
2	86	.0289	.0004	2.88	.12	76.9
3	32	.0368	.0006	3.21	.21	85.7
3	48	.0392	.0007	3.31	.17	88.4
3	64	.0411	.0007	3.34	.16	89.8
3	80	.0425	.0007	3.42	.16	91.3
4	56	.0497	.0008	3.32	.17	88.6

TABLE 13

ULTRACENTRIFUGE DATA FOR SOLUTIONS CONTAINING DAC AND .054 M NaCl

RUN	t (min)	C-CMC	σ_o	$-S/D \times 10^7$	$\sigma_{S/D} \times 10^7$	$Ma \times 10^{-3}$
5	259	.0235	.0002	1.04	.03	28.0
5	151	.0263	.0001	1.00	.03	27.0
5	87	.0291	.0002	.87	.03	23.5
5	55	.0308	.0002	.88	.04	23.8
5	55	.0396	.0002	.91	.02	24.6
5	87	.0413	.0002	.91	.02	24.6
5	151	.0441	.0003	.92	.02	24.8
5	259	.0480	.003	.91	.02	24.6

TABLE 14

ULTRACENTRIFUGE DATA FOR THE SOLUTION CONTAINING DAC AND .021 N NaCl BY THE BOTTOM DEPLETION METHOD. RUN 6

r (cm)	C-CMC	-s/D x 10^{7}	Ma x 10^{-3}
6.821	.0022	.89	24.3
6.798	.0036	.80	21.8
6.775	.0059	.80	21.8
6.752	.0096	.74	20.2
6.729	.0146	.65	17.7
6.706	.0213	.57	15.6
6.683	.0299	.49	13.4
6.660	.0385	.42	11.5
6.637	.0484	.36	9.8

TABLE 15

ULTRACENTRIFUGE DATA FOR SOLUTIONS CONTAINING DAC, NaOH* AND .1 M NaCl

RUN	t(min)	C-CMC	σ_c	$-S/D \times 10^7$	$\sigma_{S/D} \times 10^7$	$Ma \times 10^{-3}$
7	82	.0245	.0003	4.04	.10	108
7	66	.0254	.0003	3.98	.10	106
7	50	.0267	.0004	4.06	.16	108
7	66	.0411	.0005	3.72	.08	100
7	82	.0425	.0006	3.92	.11	104
8	91	.0216	.0003	4.96	.10	133
8	75	.0228	.0003	5.00	.14	134
8	59	.0239	.0004	4.93	.14	132
8	59	.0442	.0008	4.79	.12	128
8	75	.0454	.0007	4.62	.13	124
8	91	.0461	.0007	5.20	.19	139
9	466	.0212	.0003	7.38	.08	197
9	402	.0221	.0003	7.37	.07	196
9	338	.0231	.0003	7.24	.05	193
9	274	.0247	.0003	6.96	.05	186
9	210	.0251	.0003	7.27	.07	194
9	274	.0478	.0006	8.07	.10	216
9	338	.0498	.0007	8.10	.09	217
9	466	.0534	.0007	7.75	.09	207

* C_{NaOH} was .00076, .00137 and .00215 moles/dm^3 for runs 7, 8 and 9 respectively.

TABLE 16

ULTRACENTRIFUGE DATA FOR SOLUTIONS CONTAINING DMDAC AND 0.20 M KCl

RUN	t(min)	C-CMC	σ_c	$S/D \times 10^7$	$\sigma_{S/D} \times 10^7$	$Ma \times 10^{-3}$
10	82	.0240	.0003	.93	.02	20.5
10	66	.0255	.0003	.95	.02	21.0
10	50	.0271	.0003	.94	.02	20.7
10	34	.0291	.0004	.96	.03	21.2
10	18	.0327	.0004	1.01	.06	22.3
10	34	.0548	.0006	.84	.03	18.5
11	75	.0576	.0007	.83	.02	18.3
10	50	.0583	.0006	.80	.02	17.6
10	66	.0611	.0007	.80	.02	17.6
11	59	.0619	.0007	.79	.02	17.4
10	82	.0635	.0007	.79	.01	17.4
11	43	.0655	.0007	.78	.02	17.2
11	27	.0701	.0008	.78	.03	17.2
11	11	.0784	.0007	.77	.05	17.0
11	11	.103	.001	.65	.05	14.3
11	27	.112	.001	.59	.02	13.0
11	43	.118	.001	.58	.01	12.8
11	59	.123	.001	.60	.01	13.2
11	75	.127	.001	.57	.01	12.6

TABLE 17

ULTRACENTRIFUGE DATA FOR SOLUTIONS CONTAINING DMDAC AND 0.10 M KCl

RUN	t(min)	C-CMC	σ_c	$-S/D \times 10^8$	$\sigma_{S/D} \times 10^8$	$Ma \times 10^{-3}$
12	77	.0549	.0007	6.14	.13	14.2
12	61	.0580	.0007	6.32	.16	14.7
12	45	.0637	.0007	5.69	.15	13.2
12	29	.0692	.0008	5.35	.16	12.4
12	13	.079	.001	4.70	.22	10.9
12	29	.117	.001	4.20	.12	9.7
12	45	.122	.001	4.01	.09	9.3
13	130	.125	.001	4.16	.08	9.6
12	61	.128	.001	3.76	.06	8.7
12	77	.132	.001	3.64	.05	8.5
13	98	.135	.001	3.89	.08	9.0

TABLE 18

ULTRACENTRIFUGE DATA FOR SOLUTIONS CONTAINING DMDAC AND .043 M KCl

RUN	t(min)	C-CMC	σ_c	-S/D x 10^8	$\sigma_{S/D}$ x 10^8	Ma x 10^{-3}
14	133	.0509	.0005	4.31	.08	10.2
14	101	.0553	.0005	4.01	.08	9.5
14	69	.0605	.0005	3.82	.09	9.1
14	37	.0670	.0005	3.54	.11	8.4
15	111	.0746	.0004	3.41	.07	8.1
15	79	.0788	.0005	3.26	.06	7.8
15	47	.0858	.0005	3.11	.09	7.4
15	15	.098	.001	2.63	.13	6.3
14	37	.100	.001	2.44	.05	5.8
14	69	.105	.001	2.34	.03	5.6
14	101	.112	.001	2.11	.01	5.0
14	133	.117	.001	2.08	.01	4.9

TABLE 19

ULTRACENTRIFUGE DATA FOR SOLUTIONS CONTAINING TMDAC AND .10 M NaCl

RUN	t(min)	C-CMC	σ_c	-S/D x 10^8	$\sigma_{S/D}$ x 10^8	Ma x 10^{-3}
16	83	.0402	.0003	4.69	.08	12.4
16	67	.0416	.0003	4.62	.09	12.2
16	51	.0430	.0003	4.49	.09	11.9
16	35	.0448	.0003	4.61	.12	12.2
16	19	.0475	.0003	4.46	.15	11.8
16	35	.0615	.0003	3.47	.07	9.2
16	51	.0634	.0003	3.55	.07	9.4
16	67	.0652	.0003	3.47	.04	9.2
16	83	.0659	.0003	3.52	.06	9.3

TABLE 20

ULTRACENTRIFUGE DATA FOR SOLUTIONS CONTAINING DAC AND TMDAC

(X_{DAC}/X_{TMDAC} = 1) and .10 M NaCl

RUN	t(min)	C-CMC	σ_c	$-S/D \times 10^8$	$\sigma_{S/D} \times 10^8$	$Ma \times 10^{-3}$
17	82	.0503	.0004	6.13	.11	16.2
17	66	.0521	.0004	6.06	.12	16.0
17	50	.0549	.0005	6.01	.15	15.9
17	34	.0584	.0005	5.63	.15	14.9
17	18	.0627	.0005	5.44	.21	14.4
17	34	.0850	.0005	5.03	.18	13.3
17	50	.0882	.0005	4.74	.12	12.5
17	66	.0913	.0005	4.54	.08	12.0
17	82	.0936	.0005	4.48	.08	11.8

TABLE 21

ULTRACENTRIFUGE DATA FOR SOLUTIONS CONTAINING DAC AND TMDAC

(X_{DAC}/X_{TMDAC} = 2) and .10 M NaCl

RUN	t(min)	C-CMC	σ_c	$-S/D \times 10^8$	$\sigma_{S/D} \times 10^8$	$Ma \times 10^{-3}$
18	85	.0327	.0004	8.11	.13	21.4
18	69	.0343	.0004	7.98	.14	21.1
18	53	.0362	.0004	8.13	.18	21.5
18	37	.0392	.0005	7.76	.20	20.5
18	21	.0430	.0005	7.58	.27	20.0
18	37	.0653	.0005	6.55	.22	17.3
18	53	.0685	.0005	6.41	.17	16.9
18	69	.0716	.0006	6.11	.12	16.1
18	85	.0742	.0006	6.03	.10	15.9

TABLE 22

VISCOSITY DATA FOR SOLUTION CONTAINING .01798 M DAC AND .1999 M NaCl

(ρ = 1.00333 g/cc)

log ΔP	log G	Re	η (cP)
.9552	3.1649	31.8	.9043
1.2844	3.4908	67.0	.9106
1.4706	3.6761	102	.9110
1.5927	3.7980	135	.9116
1.6913	3.8974	171	.9105
1.7630	3.9683	201	.9118
1.8336	4.0390	236	.9116
1.8898	4.0954	269	.9115
1.9405	4.1461	303	.9114
2.0933	4.2984	428	.9122
2.1816	4.3877	527	.9115
2.2518	4.4575	618	.9108
2.3290	4.5359	743	.9084
2.4100	4.6161	896	.9082
2.4858	4.6921	1070	.9079
2.5670	4.7740	1290	.9068
2.6488	4.8561	1560	.9074
2.7254	4.9324	1850	.9114
2.8022	5.0071	2190	.9180
2.8794	5.0825	2590	.9198
2.9549	5.1573	3080	.9187
3.0285	5.2308	3640	.9166
3.0988	5.3027	4320	.9094
3.1691	5.3757	5130	.9008
3.2337	5.4425	6030	.8940
3.2999	5.5115	7120	.8690
3.3624	5.5773	8340	.8811
3.4515	5.6715	10400	.8727

TABLE 23

VISCOSITY DATA FOR SOLUTION CONTAINING .03639 M DAC AND .1995 M NaCl

(ρ = 1.00298 g/cc)

log ΔP	log G	Re	η(cP)
.9551	3.0553	19.1	1.1636
1.4747	3.5726	63.1	1.1654
1.6933	3.7923	105	1.1667
1.8479	3.9459	149	1.1682
1.9932	4.0911	208	1.1654
2.1610	4.2614	310	1.1568
2.2757	4.3773	405	1.1523
2.3942	4.4994	540	1.1435
2.5204	4.6282	733	1.1330
2.6292	4.7400	957	1.1274
2.7682	4.8795	1320	1.1334
2.9384	5.0464	1920	1.1352
3.1191	5.2367	3050	1.0906
3.2306	5.3623	4190	1.0484
3.3700	5.5199	6290	1.0070
3.5029	5.6665	9110	.9791

TABLE 24

VISCOSITY DATA FOR SOLUTION CONTAINING .01725 M DAC AND .2500 M NaCl

(ρ = 1.00537 g/cc)

log ΔP	log G	Re	η(cP)
.9561	3.1210	25.9	1.0025
1.2954	3.4598	56.6	1.0015
1.4738	3.6375	84.9	1.0047
1.6929	3.8557	141	1.0054
1.8709	4.0338	212	1.0041
2.0014	4.1653	287	1.0028
2.1089	4.2721	367	1.0038
2.1875	4.3512	441	1.0031
2.2556	4.4202	517	1.0073
2.3242	4.4867	601	1.0196
2.3852	4.5435	679	1.0374
2.4425	4.5944	753	1.0535
2.4889	4.6372	826	1.0528
2.5428	4.6896	926	1.0459
2.6019	4.7487	1070	1.0373
2.6829	4.8332	1300	1.0222
2.7454	4.8993	1520	1.0113
2.7990	4.9560	1750	1.0032
2.8497	5.0098	1990	.9945
2.9226	5.0886	2420	.9795
2.9936	5.1648	2930	.9669
3.0731	5.2509	3620	.9523
3.1521	5.3365	4470	.9378
3.2541	5.4475	5910	.9159
3.3624	5.5649	7950	.8941
3.4621	5.6767	10500	.8705

TABLE 25

VISCOSITY DATA FOR SOLUTION CONTAINING .02256 M DAC AND .2522 M NaCl

(ρ = 1.00527 g/cc)

log ΔP	log G	Re	η(cP)
.9560	3.0618	19.8	1.1508
1.3073	3.4077	43.5	1.1620
1.4737	3.5745	63.8	1.1581
1.5951	3.6969	84.8	1.1565
1.6944	3.7962	107	1.1574
1.7766	3.8783	129	1.1573
1.8416	3.9435	149	1.1551
1.9493	4.0528	193	1.1509
2.0323	4.1357	234	1.1553
2.1364	4.2380	294	1.1761
2.2443	4.3351	360	1.2189
2.3461	4.4240	428	1.2463
2.4546	4.5310	544	1.2278
2.5611	4.6412	709	1.1956
2.6677	4.7582	950	1.1546
2.7707	4.8741	1280	1.1176
2.8741	4.9909	1730	1.0836
2.9727	5.1017	2290	1.0553
3.0677	5.2079	3000	1.0272
3.1589	5.3109	3910	1.0006
3.2510	5.4142	5090	.9758
3.3346	5.5072	6450	.9543
3.4122	5.5938	8030	.9390
3.4640	5.6508	9260	.9316

TABLE 26

VISCOSITY DATA FOR SOLUTION CONTAINING .03577 M DAC AND .2473 M NaCl

(ρ = 1.00494 g/cc)

log ΔP	log G	Re	η(cP)
.9559	2.8820	8.65	1.7440
1.4583	3.3742	26.2	1.7818
1.6954	3.6116	45.5	1.7802
1.8338	3.7471	61.6	1.8042
1.9617	3.8674	80.3	1.8460
2.0892	3.9858	103	1.8737
2.2049	4.1012	134	1.8531
2.3193	4.2181	176	1.8152
2.4257	4.3372	239	1.7265
2.5325	4.4657	337	1.6181
2.6165	4.5691	448	1.5386
2.7762	4.7695	780	1.3989
2.9486	4.9833	1400	1.2753
3.0949	5.1634	2300	1.1853
3.3233	5.4379	4800	1.0709
3.5086	5.6593	8720	.9876

TABLE 27

VISCOSITY DATA FOR SOLUTION CONTAINING .00907 M DAC AND .2983 M NaCl

(ρ = 1.00758 g/cc)

log ΔP	log G	Re	η (cP)
.9750	3.1648	31.8	.9075
1.3031	3.5103	70.3	.9086
1.4664	3.6727	102	.9119
1.5892	3.7940	134	.9141
1.6938	3.8990	171	.9130
1.7937	3.9975	215	.9155
1.8909	4.0953	269	.9155
1.9876	4.1908	335	.9242
2.1085	4.3044	428	.9483
2.2204	4.4072	530	.9662
2.3224	4.5060	661	.9604
2.4241	4.6085	841	.9511
2.5312	4.7190	1090	.9395
2.6237	4.8159	1370	.9290
2.7285	4.9257	1790	.9174
2.8400	5.0428	2380	.9060
2.9732	5.1821	3320	.8928
3.0741	5.2890	4300	.8819
3.1764	5.3953	5550	.8715
3.2579	5.4817	6870	.8585
3.3513	5.5815	8720	.8469
3.4443	5.6818	11200	.8340

TABLE 28

VISCOSITY DATA FOR SOLUTION CONTAINING .01363 M DAC AND .2999 M NaCl

(ρ = 1.00745 g/cc)

log ΔP	log G	Re	η(cP)
.9570	3.0988	23.5	1.0573
1.3132	3.4543	53.3	1.0575
1.4795	3.6200	78.0	1.0605
1.5975	3.7371	102	1.0672
1.7017	3.8382	127	1.0860
1.8349	3.9663	167	1.1386
1.9501	4.0567	197	1.1798
2.0332	4.1312	229	1.1879
2.1053	4.2009	267	1.1785
2.1646	4.2606	306	1.1663
2.2412	4.3405	372	1.1452
2.3038	4.4081	439	1.1250
2.3750	4.4878	537	1.1021
2.4495	4.5691	659	1.0818
2.5213	4.6488	811	1.0589
2.5822	4.7168	957	1.0409
2.6554	4.7986	1180	1.0226
2.7222	4.8728	1420	1.0076
2.8024	4.9609	1780	.9903
2.8841	5.0510	2230	.9726
2.9768	5.1522	2870	.9540
3.0657	5.2496	3670	.9364
3.1736	5.3676	4920	.9173
3.2561	5.4560	6110	.9047
3.3297	5.5352	7440	.8902
3.4595	5.6793	10700	.8608

TABLE 29

VISCOSITY DATA FOR SOLUTION CONTAINING .01815 M DAC AND .3017 M NaCl

(ρ = 1.00731 g/cc)

log ΔP	log G	Re	η (cP)
.9569	2.9972	14.7	1.3346
1.2924	3.3380	32.7	1.3324
1.5030	3.5442	52.0	1.3404
1.5936	3.6291	62.4	1.3724
1.6875	3.7147	74.5	1.4167
1.7445	3.7629	81.8	1.4448
1.7961	3.8103	90.3	1.4457
1.8675	3.8768	104	1.4502
1.9187	3.9260	116	1.4429
1.9853	3.9940	136	1.4217
2.0453	4.0571	158	1.4000
2.1126	4.1302	189	1.3700
2.1908	4.2177	237	1.3292
2.2505	4.2869	284	1.2965
2.3115	4.3569	341	1.2686
2.3704	4.4248	407	1.2405
2.4331	4.4987	494	1.2091
2.4919	4.5675	593	1.1772
2.5562	4.6440	727	1.1508
2.6194	4.7138	872	1.1384
2.6820	4.7855	1050	1.1116
2.7461	4.8592	1270	1.0886
2.8175	4.9402	1560	1.0663
2.8890	5.0212	1930	1.0459
2.9536	5.0937	2310	1.0301
3.0090	5.1550	2700	1.0135
3.0868	5.2430	3380	.9885
3.1845	5.3544	4510	.9593
3.2801	5.4614	5930	.9356
3.3692	5.5600	7610	.9163

TABLE 30

VISCOSITY DATA FOR SOLUTION CONTAINING .02268 M DAC, .2509 M NaCl AND .0003903 M NaOH (ρ = 1.00571 g/cc)

log ΔP	log G	Re	η(cP)
.9562	3.0168	16.1	1.2768
1.2877	3.3451	34.0	1.2820
1.4659	3.5250	51.7	1.2750
1.5996	3.6580	70.2	1.2820
1.6907	3.7481	86.5	1.2908
1.7743	3.8286	103	1.3089
1.8389	3.8890	117	1.3308
1.9487	3.9871	143	1.3797
2.0348	4.0617	165	1.4139
2.1402	4.1578	202	1.4188
2.2457	4.2651	259	1.3834
2.3500	4.3785	344	1.3341
2.4585	4.5018	472	1.2779
2.5637	4.6242	652	1.2228
2.6702	4.7479	903	1.1733
2.7728	4.8676	1240	1.1305
2.8763	4.9871	1690	1.0929
2.9749	5.0997	2260	1.0605
3.0695	5.2072	2990	1.0284
3.1577	5.3087	3880	.9992
3.2434	5.4058	4990	.9758
3.3265	5.4986	6320	.9521
3.4149	5.5993	8180	.9253
3.4665	5.6583	9570	.9107

TABLE 31

VISCOSITY DATA FOR SOLUTION CONTAINING .02257 M DAC, .1516 M NaCl AND .0996 M HCl (ρ = 1.00350 g/cc)

log ΔP	log G	Re	η(cP)
.9553	3.0595	19.5	1.1543
1.2928	3.3933	41.9	1.1617
1.4723	3.5727	63.4	1.1603
1.5999	3.7005	84.9	1.1593
1.6970	3.7985	106	1.1555
1.7735	3.8758	128	1.1549
1.8384	3.9405	148	1.1560
1.8965	3.9990	170	1.1540
1.9460	4.0488	191	1.1544
2.0328	4.1347	232	1.1629
2.1038	4.2041	271	1.1805
2.1906	4.2820	318	1.2203
2.2876	4.3653	373	1.2558
2.3800	4.4505	447	1.2548
2.4676	4.5402	550	1.2286
2.5618	4.6405	705	1.1937
2.6673	4.7574	950	1.1532
2.7708	4.8746	1270	1.1153
2.8738	4.9912	1730	1.0804
2.9721	5.1026	2300	1.0498
3.0675	5.2095	3023	1.0225
3.1569	5.3106	3920	.9960
3.2435	5.4083	5030	.9713
3.3264	5.5008	6370	.9493
3.4055	5.5893	7950	.9290
3.4656	5.6575	9500	.9137

APPENDIX A

Sample Analysis of Archibald Data - A solution which was initially 0.0986 M in DMDAC and 0.1024 M in KCl was centrifuged for over 80 minutes at a rotational speed of 36,000 revolutions per minute. Among the photographs acquired was one at 61 minutes using a phase plate angle of 110°. A small amount of an inert fluorocarbon in the sample sector served to elevate the "no flux" interface from the physical bottom of the cell. This practice ensures that the interface will form along the bottom of a cylindrical volume element.

The data obtained by measuring the deflection of the Schieren image from a base line image formed by water in the reference sector of a double sector cell was used to obtain the concentration gradient of surfactant at each radial position using a value of 0.154 for the specific refractive index increment. Apparent values for the concentration and Archibald variable were calculated by applying the usual expressions[19] to the data from the plateau region, where $dc/dr = 0$, to each radial position as if that position were the "no flux" interface. These values, which are listed in table 32 were extrapolated in the log plots shown in figure 13 to the actual interface to obtain values of $6.32 \pm 0.16 \times 10^{-8}$ and 0.0580 ± 0.0007 for the Archibald variable and molar concentration respectively. Multiplication of the former

by $RT/(1-\rho\bar{v})$ results in an apparent molecular mass, Ma, of 14.7×10^3 g mol^{-1}. The result of this analysis is included in table 17 and figure 6.

TABLE 32

ANALYSIS OF DATA ABOUT THE BOTTOM INTERFACE FROM PHOTOGRAPH TAKEN 61 MINUTES AFTER START OF CENTRIFUGE RUN 12

[1] r (cm)	[2] Δr (cm)	-dC/dr (M cm^{-1})	[3] C (M)	[3] $-(2/\omega^2)\,d\ln c/dr^2 \times 10^8$ (rad^2 s^{-2} cm^{-2})
7.0808	.0148	.3388	.0666	5.08
7.0692	.0263	.3170	.0702	4.51
7.0577	.0378	.2959	.0737	4.02
7.0462	.0494	.2704	.0769	3.53
7.0346	.0609	.2474	.0798	3.11
7.0291	.0724	.2233	.0825	2.72
7.0116	.0840	.1999	.0849	2.37
7.0000	.0955	.1775	.0870	2.06
6.9885	.1070	.1545	.0889	1.76
6.9770	.1186	.1365	.0905	1.53
6.9654	.1301	.1179	.0920	1.30
6.9539	.1416	.1014	.0932	1.10
6.9424	.1532	.0870	.0943	.94
6.9308	.1647	.0712	.0952	.76
6.9193	.1762	.0593	.0959	.63
6.9078	.1878	.0480	.0965	.51
6.8962	.1993	.0394	.0970	.42
6.8847	.2108	.0321	.0974	.34
6.8732	.2224	.0261	.0977	.27
6.8616	.2339	.0223	.0980	.23
6.8501	.2454	.0172	.0983	.18

continued ....

TABLE 32 (continued)

[1]r(cm)	[2]Δr(cm)	-dC/dr(M cm^{-1})	[3]C(M)	[3]$-(2/\omega^2)$dlnc/dr^2 x 10^8 (rad^2 s^{-2} cm^{-2})
6.8386	.2570	.0141	.0984	.14
6.8270	.2685	.0116	.0986	.12
6.8155	.2800	.0086	.0987	.09
6.8040	.2916	.0071	.0988	.07
6.7924	.3031	.0047	.0988	.05
6.7809	.3146	.0023	.0989	.02
6.7693	.3262	0	.0989	0

[1]Radial displacement from centre of rotation.

[2]Displacement from interface.

[3]Values in these columns are derived from the proceedure outlined in the text. Only the value extrapolated to the real interface has physical significance.

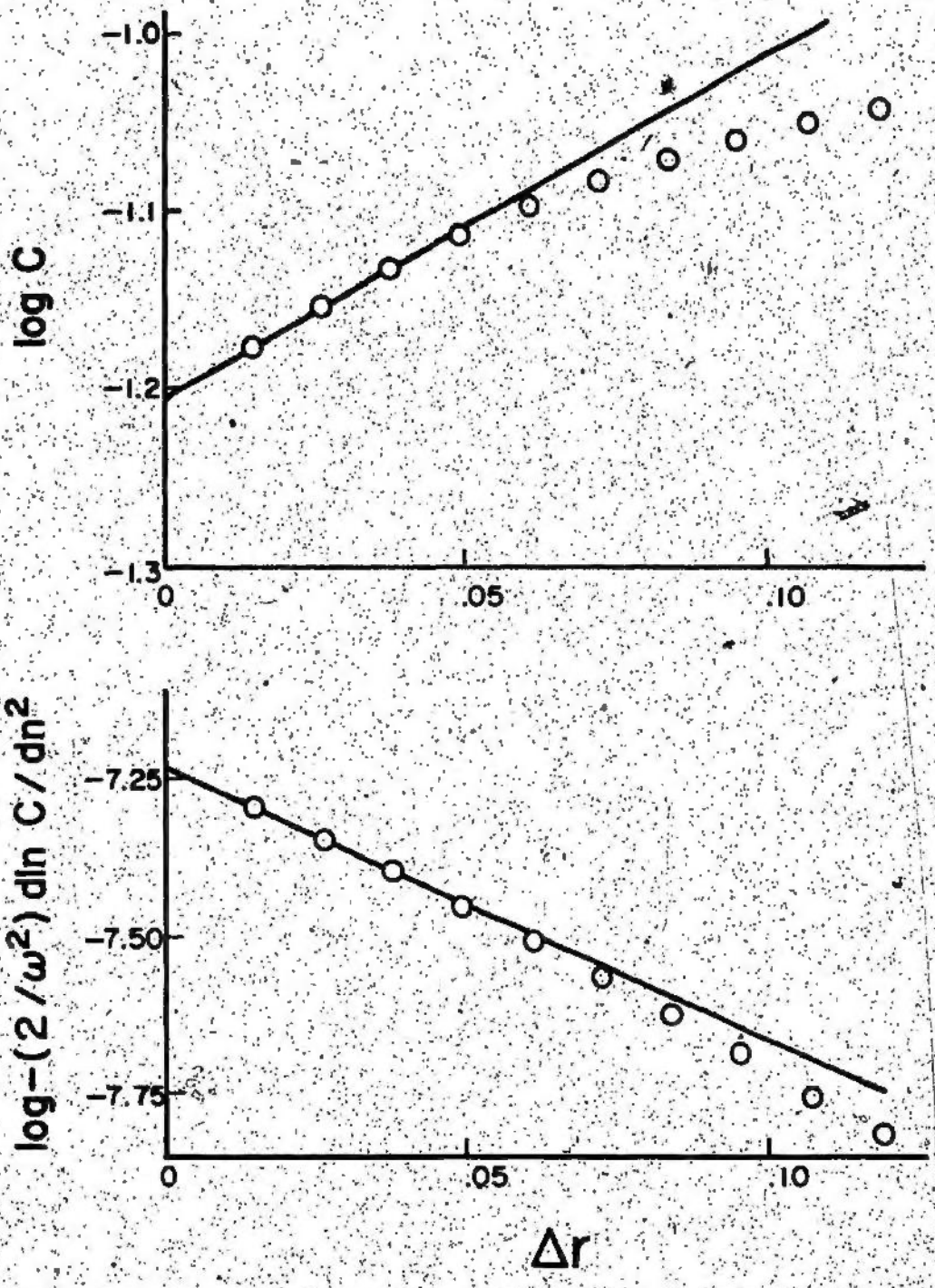

Figure 13 Plots showing typical extropolations of data from an Archibald type experiment. Data from table 32.